Geophysical Surveys in the Harshaw Creek Area, Patagonia Mountains, Arizona

Geophysics Field Camp 2020

Laboratory for Advanced Subsurface Imaging

LASI-20-1

August 1, 2020

Kate Willa Brown, Ryan A. Harris, Harrison C. Russell,

Ben K. Sternberg, Zida Wang, Dania Xavier

Abstract

Over the weekends of February 15-16 and 22-23, 2020 geophysical data were collected by students from the University of Arizona in cooperation with the US Geologic Survey. The survey was conducted in the Lower Harshaw Creek area of Patagonia, Arizona. The objective of this survey was to define features of the setting for surface water and groundwater across three ranch properties that had varying levels of potable water. Local mineralization in the area led to high concentrations of dissolved solids and low pH in certain wells. DC Resistivity and Transient Electromagnetic were the primary methods used in the survey, with the GEM-2 Frequency Domain Electromagnetic system used in a smaller portion of the survey. These methods allowed for subsurface mapping of the study area with respect to local resistivities. The results of these surveys determined that the likely cause of the varying potability was a shallow rock body containing a high percentage of sulfide minerals. The local geology and nearby area's mineral occurrences suggest the observed anomalies can best be explained as a buried skarn or epithermal base metal vein-type mineralization. This deposit lies within a shear zone, which caused an uplift of the body under certain sections of the survey area. This zone with the sulfide rich body is the leading theory for the occurrence of non-potable groundwater in the survey area.

Table of Contents

Acknowledgements

The University of Arizona Field Geophysics class (GEN/GEOS 416/516), would like to thank the United States Geological Survey (USGS) for providing funding and support for this project. Jamie Macy has played a vital role in our Geophysics Field classes for many years, providing the required equipment and processing the data. Lucien Bucci from the USGS was with us during all the surveys and educated the class about the instrumentation, field procedures, and safety in the field. We would like to thank Floyd Gray from the USGS for giving us a detailed introduction to the area and the project before our first weekend in the field. Floyd was also in the field with us during the entire survey and educated the class about correlating geophysics results with geologic and hydrologic information. Without the assistance of the USGS this project would not have been possible. All of us who were in the field would like to thank Chris Peterson for allowing access to the field survey area, for her knowledge of the area, and for her generous hospitality. Finally, we would like to thank Zonge International for their 34 years of support of this class as well as providing important information for the report and presentation.

1. Introduction

1.1 Project History and Objectives

The area of focus for this study follows the approximately 1 kilometer stretch of Harshaw Creek that runs along the southwestern base of Red Mountain, about 5 kilometers east of the Town of Patagonia, Arizona. A handful of ranch properties are occupied and operate out of the Harshaw Creek valley system. These ranches rely primarily on groundwater supplied by well pumps to sustain the human and animal residents alike. The properties all have a clean, potable groundwater supply apart from Red Rock Ranch.

The U.S Geological Survey (USGS) has been studying the Harshaw Creek area to map the geology and water table of the area and to investigate possible causes of this anomalous and isolated contamination of groundwater. Up to five wells have been drilled on the Red Rock Ranch property to use for drinking water and for cattle ranching; all were discovered to produce water with a pH as low as 3.5 and dangerously high metal concentration. The chemistry of the stream water within Harshaw Creek and the well water of the surrounding ranch properties has been tested by the USGS as well and was found to be within typical healthy limits. As the variation in groundwater quality appears to occur in the zone isolated to the one property, geophysical surveys spanning the boundaries between Red Rock Ranch and the nearby properties were proposed to investigate the physical properties of subsurface layers and to interpret the lithologic structure and its spatial variation.

To aid in the investigation, the USGS asked the GEOS/GEN 416/516 class from the University of Arizona to conduct geophysical surveying of the land to help locate and understand the interaction of the water with the geology. The survey methods used to infer the subsurface structure utilize electric current to map the variations of electrical resistivity in the earth. The GEM-II, the direct current (DC) resistivity array, and transient electromagnetic (TEM) loop surveys used in this investigation are intended to map the resistivity at different resolutions, depths, and distances along the same transect. As these methods all have their own strengths and

weaknesses and provide information better suited for certain interpretations, a comparison of data for the same area from all three techniques will allow for more accurate and objective interpretations.

1.2 Geologic background

The Patagonia Mountains have a long history of mining, with the earliest records showing the ancestors of the Papago Indians working the area in the 16th century (Schrader & Hill, 1915) . This has continued through to the present day with the Hermosa mine, owned by South32, expecting to finish pre-feasibility studies by the end of 2020. The deposit is a zinc-lead-silver sulfide rich body. The major geological units in the area are Lower-Permian carbonates atop of Cambrian sediments and Pre-Cambrian granodiorites. Sitting unconformably above the Carbonates are Mesozoic, Laramide associated, volcanic rocks and batholiths (Figure 2.1).

Low grade silver mineralisation occurs within the intermediate and felsic Mesozoic volcanic rocks. Epithermal veins and silicified fault breccia are also enriched and provided the source of the historic silver mined here long ago. Skarn type and base metal sulfide replacement veins are found along the contacts of the Permian carbonates and the Laramide associated intrusive rocks (Chatman, 1994).

Structural trends align on a NW bearing. The faulting is a mixture of normal and thrust, due to the originally contractional and later extensional nature of the North America Cordillera. Due to the Farallon slab and associated mid ocean ridge being completely subducted beneath the North American plate, original contraction turned to extension as the San Andreas Fault evolved (DeCelles et al., 2009).

1.3 Hydrology

Harshaw Creek is a part of the Sonoita Creek Basin and is tributary to the Santa Cruz River Watershed. In the project area the creek flows approximately to the northwest. The streamflow within the creek is ephemeral and relies on the contribution of surface flow from the basins upstream and a perennial spring. The creek's primary tributary basins to the southeast provide runoff to the creek during periods of precipitation and snowmelt. These basins are mostly untouched by human development except for the canyon containing the Endless Chain Mine. During periods of baseflow in which there is no influx of surface water, the spring is the only constant source of streamflow. While the creek is at baseflow the water in the creek is observed to disappear into the alluvium within ~100 meters from the source (Proposal of a Total Maximum Daily Load For: Upper Harshaw Creek, Sonoita Creek Basin, Santa Cruz River Watershed, Coronado National Forest, near Patagonia, Santa Cruz County, Arizona, 2003).

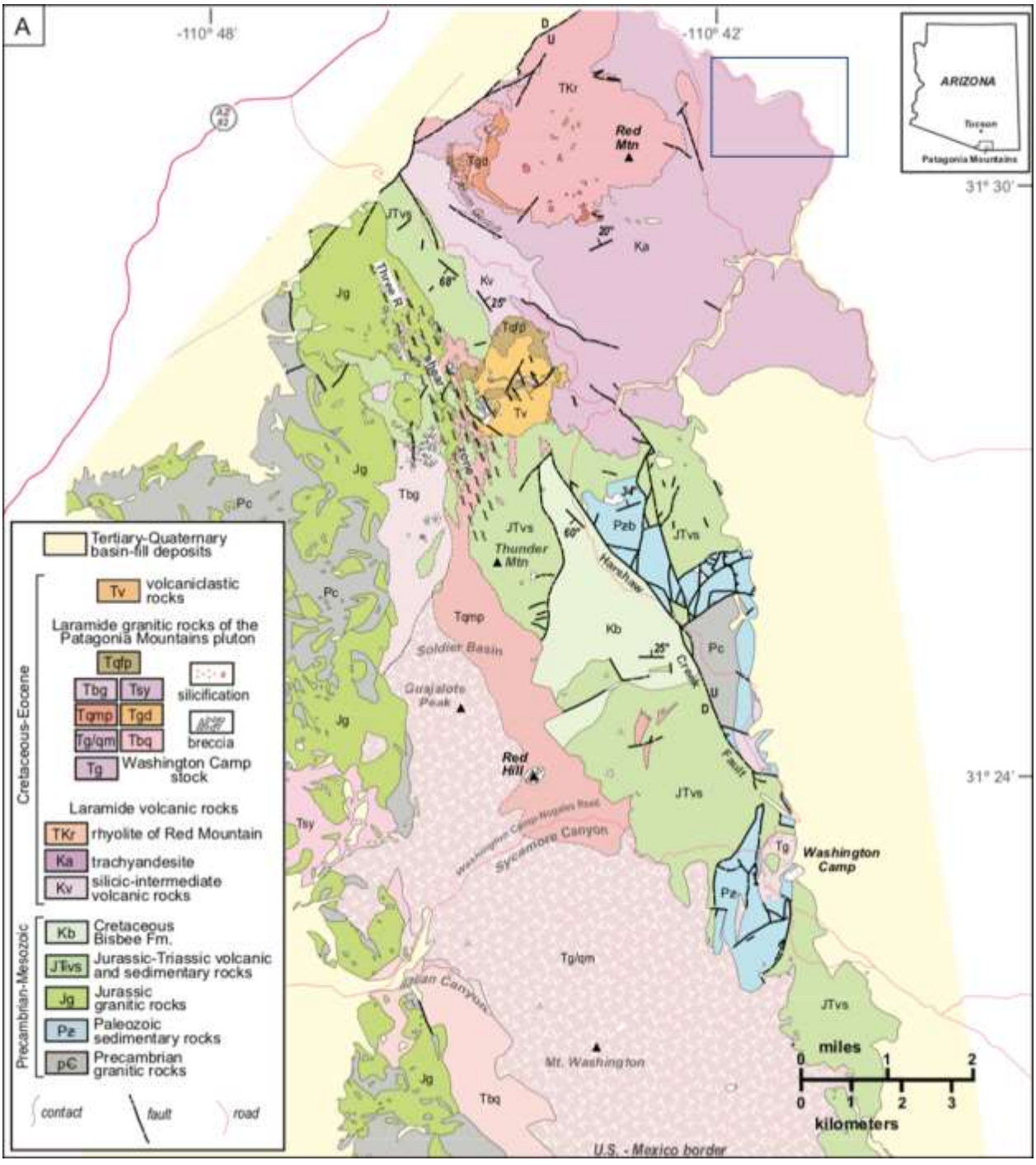

Figure 2.1. A geological map of the Harshaw Creek area made by (Vikre et al., 2014)). The site for this study is highlighted by the blue box in the NE corner.

1.4 References

Chatman, M. L. (1994). *Patagonia Mountains-Canelo Hills Unit, Cochise and Santa Cruz Counties, Arizona* (Mineral appraisal of the Coronado National Forest No. 7) (p. 392). U.S Department of the Interior Bureau of Mines.

DeCelles, P. G., Ducea, M. N., Kapp, P., & Zandt, G. (2009). Cyclicity in Cordilleran orogenic systems. *Nature Geoscience*, *2*(4), 251–257. https://doi.org/10.1038/ngeo469

Proposal of a Total Maximum Daily Load For: Upper Harshaw Creek, Sonoita Creek Basin, Santa Cruz River Watershed, Coronado National Forest, near Patagonia, Santa Cruz County, Arizona. (2003, June 30). *Arizona Department of Environmental Quality*, Retrieved May 10, 2020, from http://www.patagoniaalliance.org/wp-content/uploads/2013/12/ADEQHarshawCreek.pdf

Schrader, Frank. C., & Hill, James. M. (1915). *Mineral Depostis of the Santa Rita and Patagonia Mountains Arizona* (No. Buletin 582) (p. 395). USGS.

Vikre, P. G., Graybeal, F. T., Fleck, R. J., Barton, M. D., & Seedorff, E. (2014). Succession of Laramide Magmatic and Magmatic-Hydrothermal Events in the Patagonia Mountains, Santa Cruz County, Arizona. *Economic Geology*, *109*(6), 1667–1704. https://doi.org/10.2113/econgeo.109.6.1667

2. Location Maps

2.1 Geographic Location and Background Information

The study area is in the southeastern Santa Rita and northern Patagonia Mountains as shown in Figures 2.1. and 2.2. Our data collection was done in the lower Harshaw Creek area, on the Red Rock Ranch, and Peterson Homestead. In order to keep our profile lines location consistent, and to record the coordinates for each geophysical method stations, we used a Garmin GPSMAP 64st GPS unit, the GPS compass and location markers. The data were processed using Google Earth Pro, and ArcGIS pro. We used UTM coordinate system and our data falls in the 12R zone; with eastings ranging from 527854.8 to 52907.05, and northings ranging from 348706.34 to 3487711.24. Table 2.1 gives a key for the names and units used in this report.

Name	Key
RRR	Red Rock Ranch
HC	Harshaw Creek
DC Resistivity	Direct Current Resistivity
TEM Loops	Transient Electromagnetics Loops

Table 2.1. Summary Key of terms used in the report.

The elevation data were acquired by multiple Garmin 64st GPS units, and Google Earth Pro which proved to be the most reliable elevation source. Elevation profiles were produced by Jamie P. Macy, USGS, Flagstaff.

2.2 Geophysical Survey Locations

DC Resistivity lines were laid for both RRR and HC locations. The HC DC Resistivity line was about 421m long, while the RRR DC Resistivity line was about 514 m long; the lines consisted of 56 electrodes per array with a 4m spacing between each of them. Figures 2.6 and 2.7 show the exact locations of each of the DC lines; the electrodes are represented by red dots numbered every 50 stations.

For the TEM surveys, we had 20 x 20m transmitter loops laid out and directed from East to West

for both study areas. In the RRR area fifteen loops were laid out. The HC area had fourteen transmitter loops laid out. In addition, in order to minimize disruption due to ground vegetation and unreasonably steep terrain, some of the TEM loops were shifted from the center line, and to avoid interference from nearby metallic fences the loops were set 20 m away from fences. Figures 2.7 and 2.8 show the exact location, station numbers and distribution of the TEM survey loops for both study areas.

2.3 Geologic Map

Before performing and interpreting the geophysical survey data, it is important to understand the geology of the site. This provides a better understanding of the mineral composition and geological alterations that took place in the area, and from which we may draw hypotheses of its impact on the hydrology in the area. Basic Geological maps illustrating the geological formations within the study were provided by Floyd Gray, USGS, Tucson, including an assessment of the pH-water quality as shown in Figure 2.3. The Lower Harshaw Creek area is located over Cretaceous Volcanic rocks (Kv) from the upper cretaceous. Figure 2.4 gives a basic illustration of the type of rocks (un-altered basalt and altered rock) within the RRR and HC study areas.

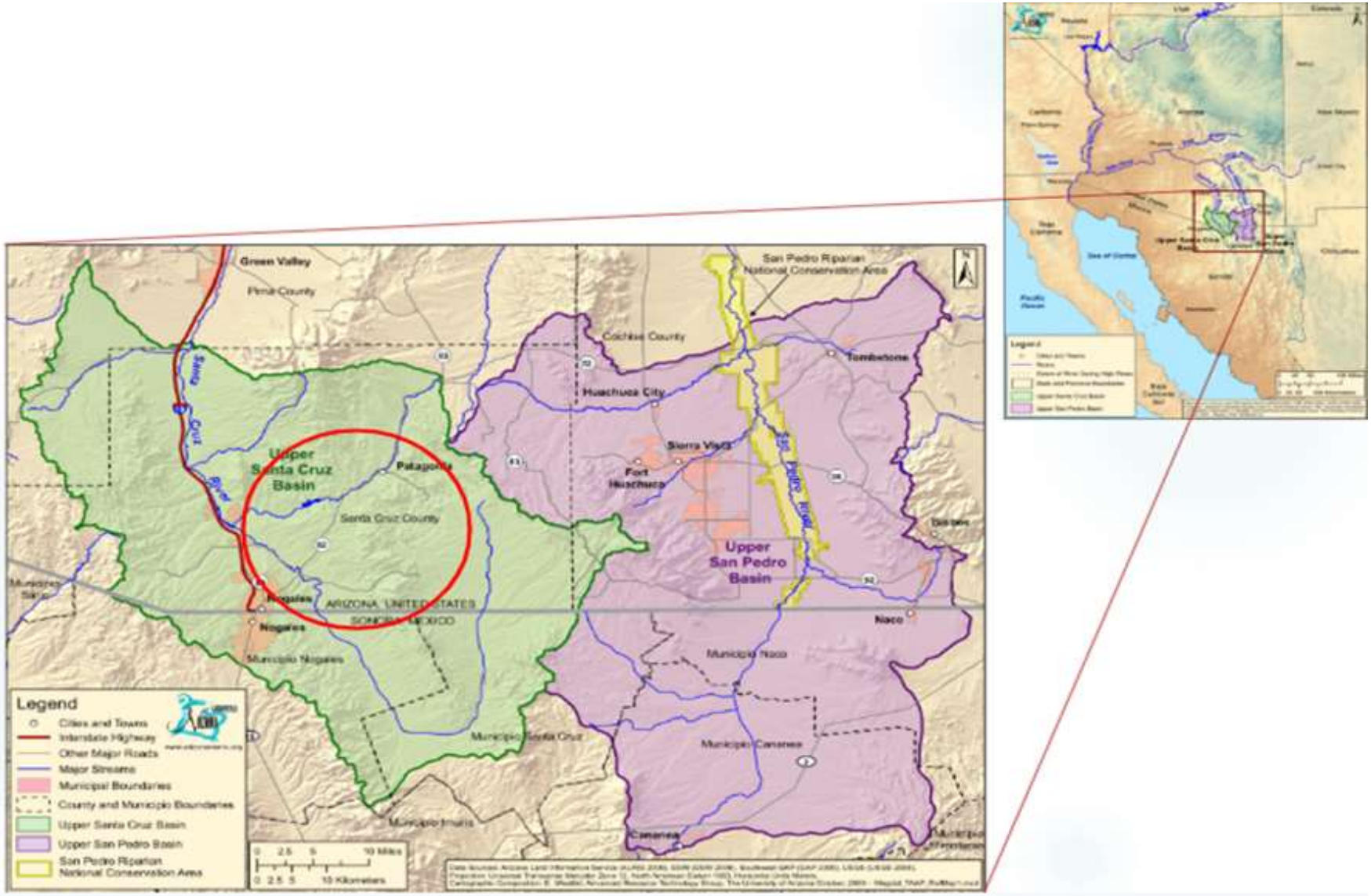

Figure 2.1. Study Area in the Patagonia Mtns, Courtesy of Floyd Gray.

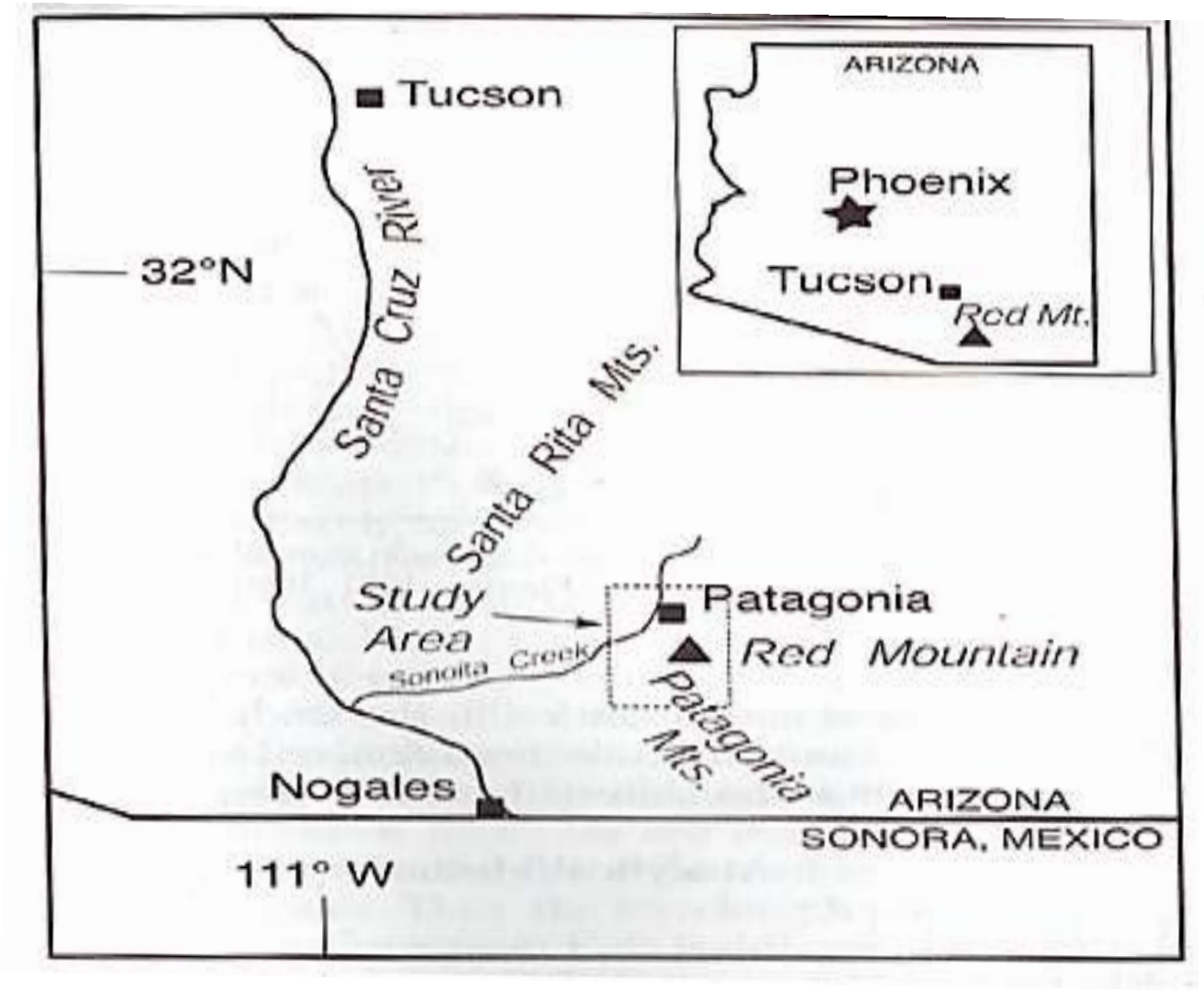

Figure 2.2. Location of the study area: Southeastern Santa Rita and Northern Patagonia Mountains. Courtesy of Floyd Gray.

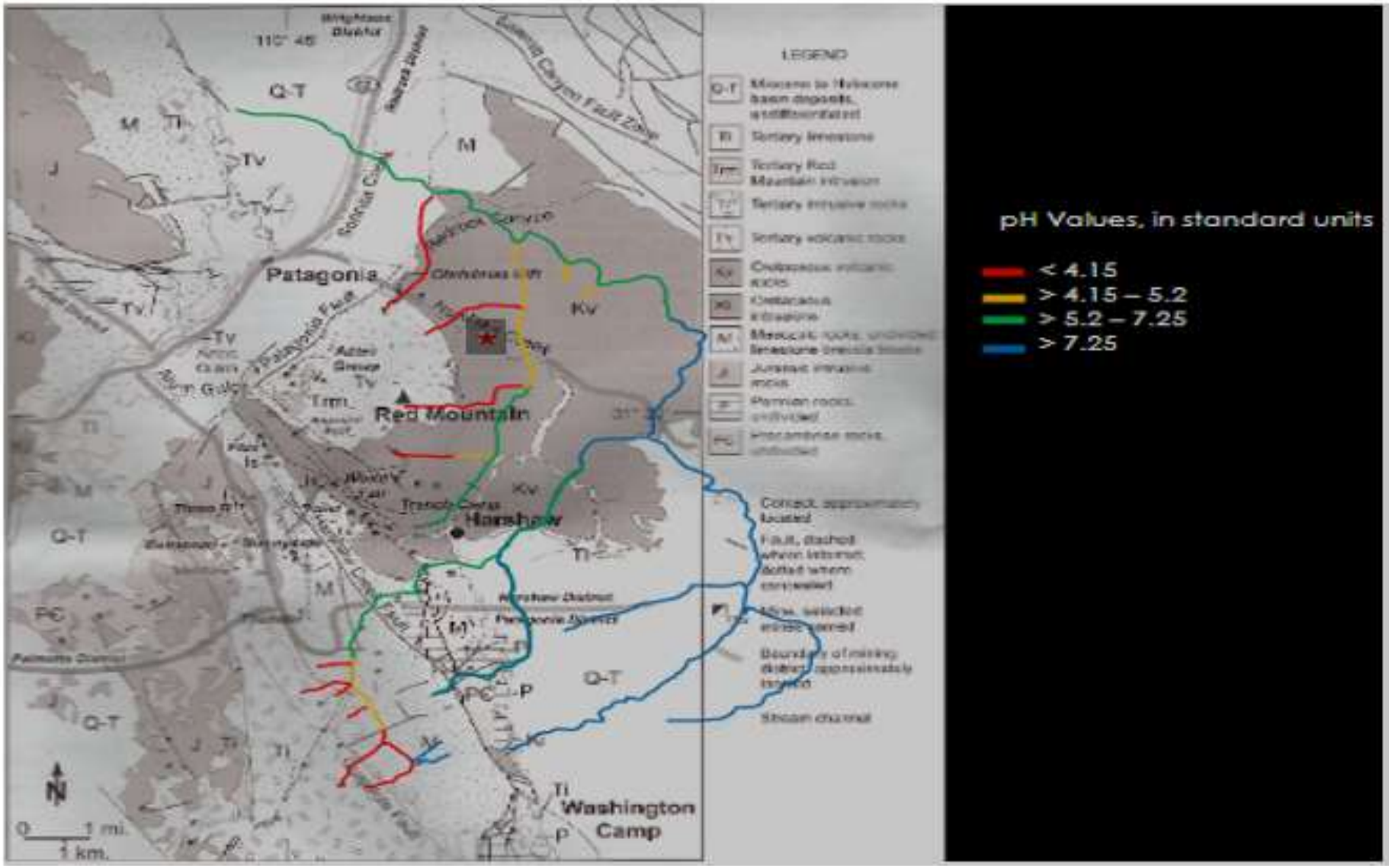

Figure 2.3. Generalized geologic map of the southeastern Santa Rita and the northwestern Patagonia Mountains (modified from Simons, 1974; Drewes, 1971, 1980); and pH-Water quality Assessment parameter. Courtesy of Floyd Gray.

Figure 2.4 Basic Illustration of the rock type within the study area (b- basalt, ar- altered rock). Courtesy of Floyd Gray.

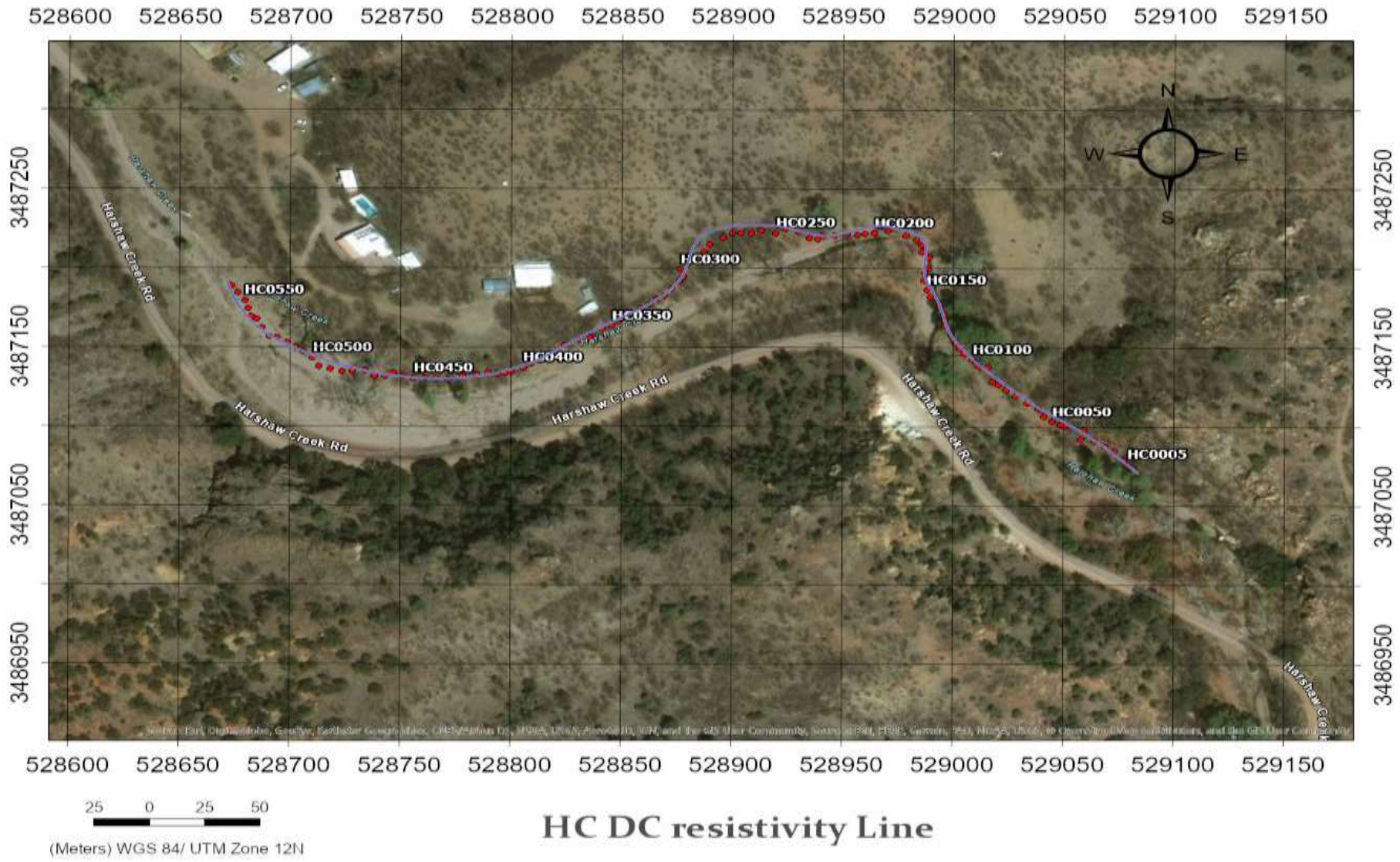

Figure 2.5. Location map for the HC DC Resistivity line.

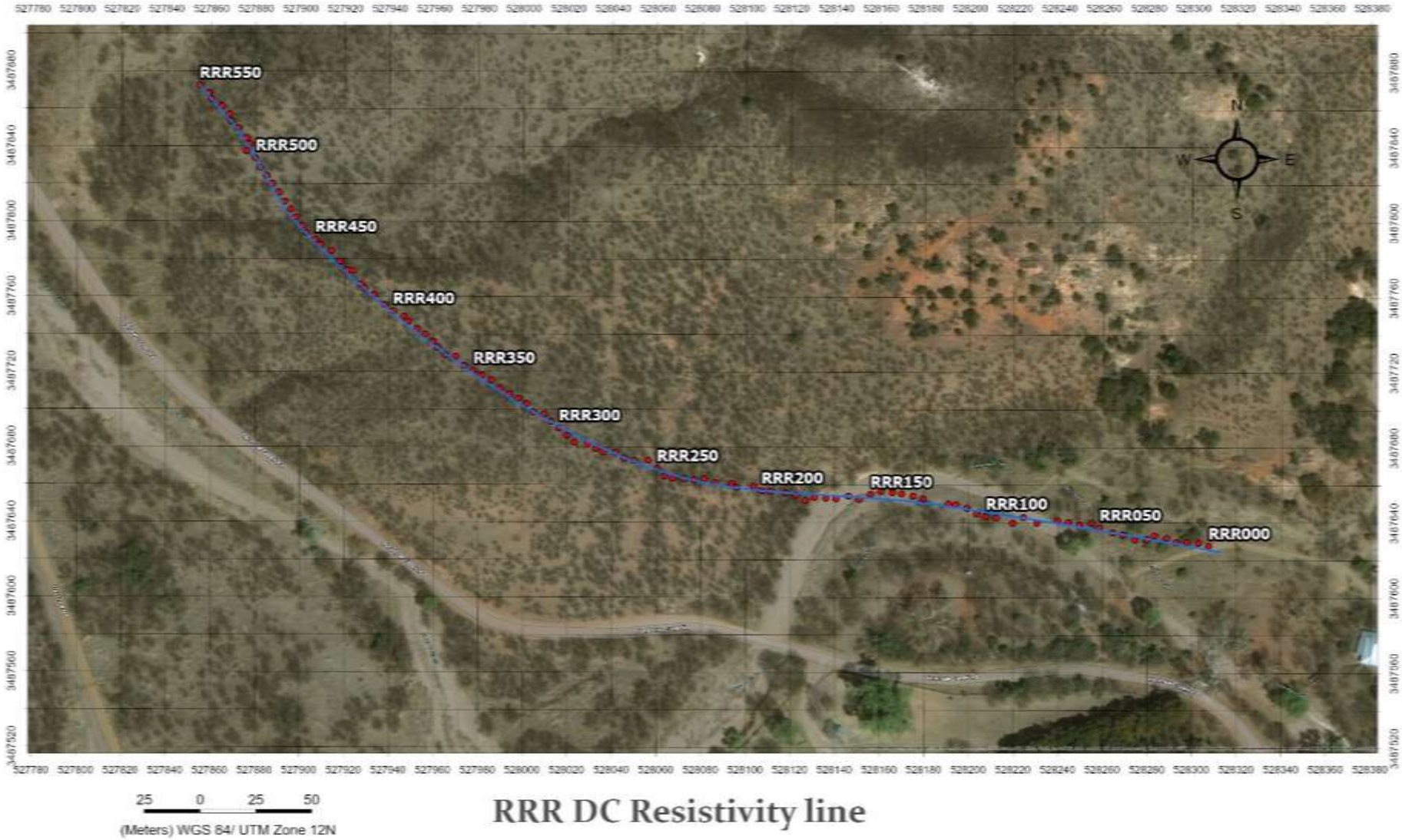

Figure 2.6. Location map for the RRR DC Resistivity line.

Figure 2.7. Location map for the RRR 20 m TEM Loop.

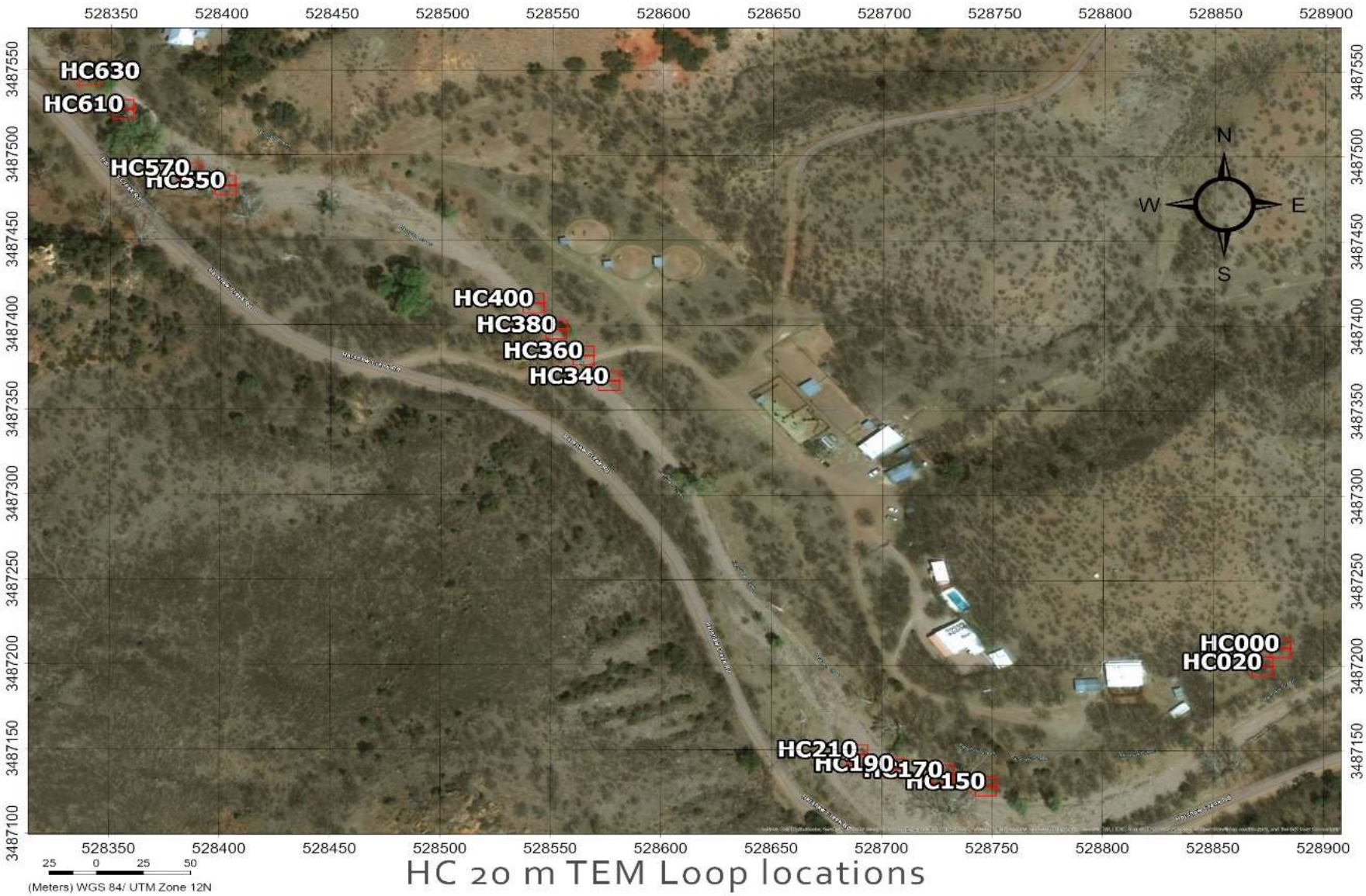

Figure 2 8. Location map for the HC 20 m TEM Loop.

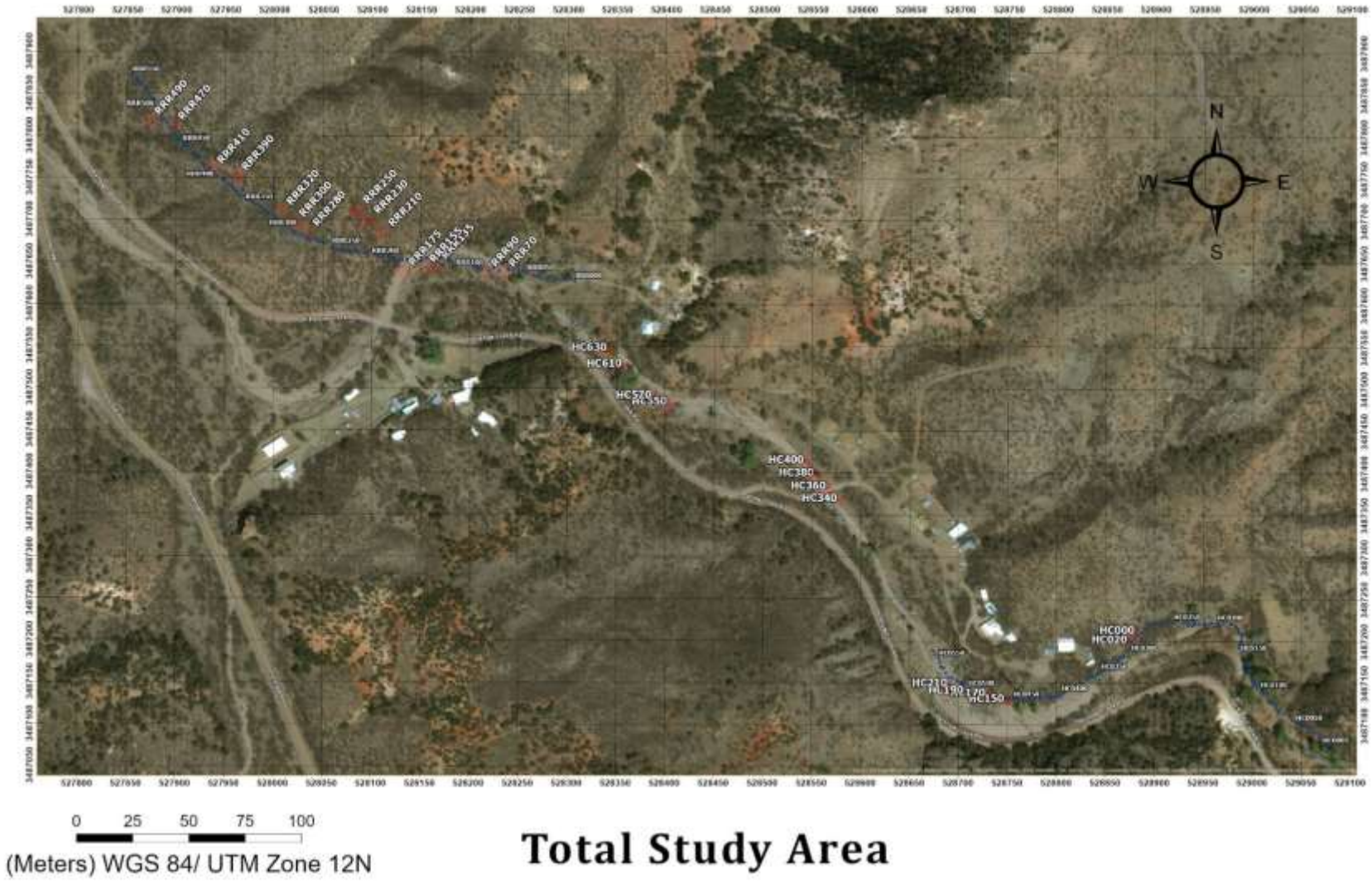

Figure 2.9 Location map of total study area.

2.4 References

Gray, Floyd, 2020, Advanced Geophysical Field Techniques - Red Rock Ranch-Peterson Homestead. PowerPoint Presentation to the GEN/GEOS 416/516 class on January 2020.

3. Transient Electromagnetic (TEM) Surveys

3.1 Introduction

The transient electromagnetic (TEM) method is a geophysical technique that provides information on the electrical resistivity of the subsurface. A loop of insulated wire is laid on the ground over a target area, which acts as a transmitter, and is driven by a time varying current (Figure 3.1). “The change in current and the resulting EM field establish an image current within the earth equal in magnitude, but opposite in polarity, to that of the transmitter” (Zonge, 2018). Conductive material in the earth below interacts with the image current to create secondary magnetic fields which are then measured at the receiver. The depth of exploration depends on the transmitter loop size, with one to three times the loop size being an acceptable guideline for reliable data. “The TEM method is based on transmitting a time-domain, square-wave signal into a large, ungrounded wire loop and then interrupting the current as fast as possible causing a rapid change in the magnetic field.” (Zonge, 2018) This produces currents in surrounding conducting materials, forming small secondary magnetic fields that are observed in the induced voltages in receiver loops. These induced currents decay rapidly in material with poor conductivity (moderate resistivity) and slowly in material with good conductivity (low resistivity). Material with very poor conductivity (high resistivity) cannot sustain any quantifiable induced currents. Modeling software is then used to convert TEM measurements to profiles of resistivity vs depth. This is then used to help identify changes in the subsurface.

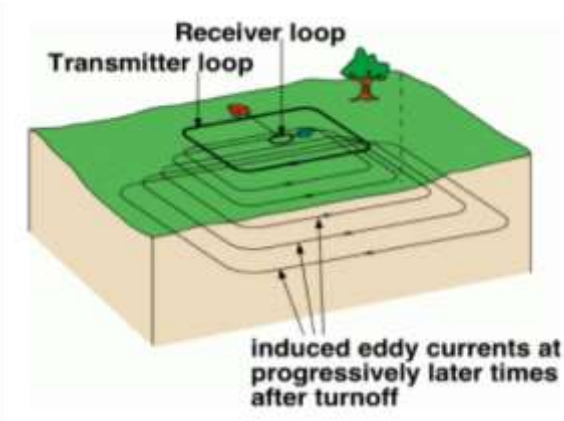

Figure 3.1. Representation of a TEM setup showing the transmitter and receiver loop (Zonge, 2020).

3.2 Instruments and Field Procedures.

The instruments that were used in this survey are a Zonge International GDP-32 II receiver with the Zonge International NT-20 transmitter, which together are known as the Zonge NanoTEM system. (Figures 3.2 and 3.3). The GDP-32 II can be used to measure TEM transients at short time delays. The TEM measurements provide information about the subsurface.

Figure 3.2 Zonge International GDP-32 II.

Figure 3.3 Zonge International NT-20.

The measurement parameters were: Loop Size = 20 X 20meters, Transmitter Ramp Time = 305 uSec, Repetition Rate = 32 Hz, Receiver Loop Size = 5m X 5m.

The data were collected on two days, February 16th, 2020, and February 22nd, 2020. TEM data were collected after the DC Resistivity survey data and ran closely along the same line, so the data could be compared between the two. The set up consisted of two squares, referred to as loops. A 5x5 meter receiver loop was placed in the middle of the 20x20 meter transmitter loop (Figure 3.1). Depth was to be anticipated at approximately 1 to 3 times the length of a side of the transmitter loop. The team sharing the duties of equipment setup, consisted of seven students, and one U.S.G.S. personnel.

Two lines of multiple TEM loops were measured from East to West. Line one consisted of thirteen loops starting at the Patterson Ranch, and ending at an adjacent property,

called the Red Rock Ranch line (Figure 3.4). Between loops 10 and 11, a fence was skipped to avoid any disruptions in the soundings. Line 2 consisted of fourteen loops trending from East to West. The line started four hundred meters East of Red Rock Ranch (Figure. 3.6). The line started at loop 0 and ended at loop 14. The areas between TM 20 and TM150 were avoided because of a metal fence. The second area avoided was between TM400, and TM 550, because of another fence. All precautions were taken to avoid disruption of the soundings.

3.3 Data Processing

All TEM data collected in the field, and all location information are shown in Figures 3.4 through 3.7. The data were downloaded from the GDP-32 II and the Zonge software TEMAVG was used to average the TEM measurements. At each site there are at least 3 measurements; we took an average of all 3 measurements. After averaging the data, we used another Zonge program called Smooth TEM inversion (STEMINV). This software inverts the data collected from the field by fitting a layered-earth model to produce the earth model. After this, we applied the output from STEMINV to another Zonge program called MODSECT. This visualization software helped us to make a cross-section with those data. After that, we put the output from MODSECT in a program called Surfer, made by Golden software. Figure 3.5 and 3.8 are the output of Surfer, which is our final output of those data. All data processing for these data sets was done by Jamie Macie at the USGS in Flagstaff, Arizona.

3.4 Archie's Equation

In order to interpret the data and cross-sections obtained from the TEM survey, there is an important equation that needs to be understand, i.e. Archie's Law (or Archie's Equation). Archie's law is an empirical relationship between the effective rock resistivity and the porosity of the rocks and the volume fraction of pores with water. Based on Archie's Law (Equation 3.1), where ρ is effective rock resistivity, ρ_w is the

resistivity of the porewater; φ is the porosity; s is the volume fraction of pores with water; a, m, n are constants where $0.5 \leq a \leq 2.5$, $1.3 \leq m \leq 2.5$, and $n \approx 2$, (Reynolds, 2011).

$$\rho = a\varphi^{-m}s^{-n}\rho_w \qquad 3.1$$

Based on this equation, rock and soil with higher porosity or volume fraction of pores containing water, will lead to a lower rock resistivity. Applying this equation to the cross-sections, Figures 3.5 and 3.7, the lower resistivities on the cross-sections indicate higher water concentration.

3.5 Data

3.5.1 Location maps and cross-sections for Red Rock Ranch

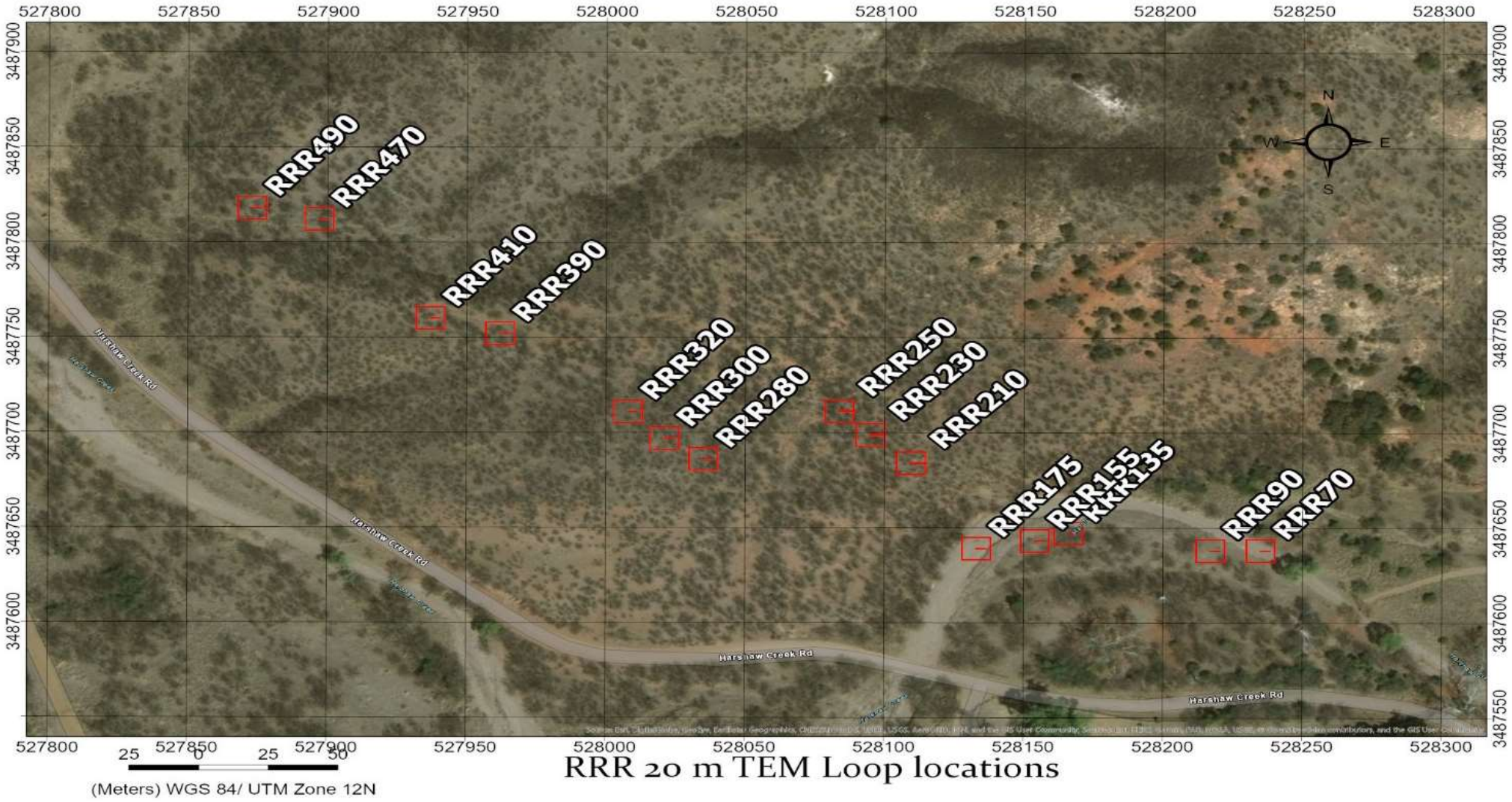

Figure 3.4. Red Rock Ranch TEM Location Map with loop Size 20m

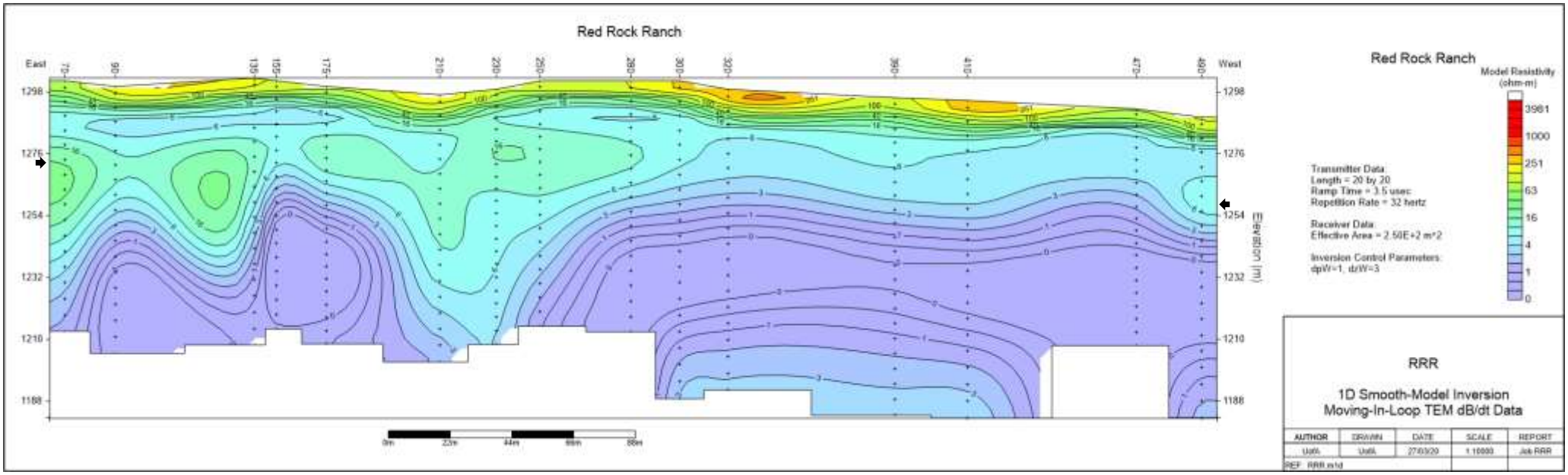

Figure 3.5. Red Rock Ranch TEM model with elevation data, 20m loop. Note warm colors indicate high resistivity and cool colors indicate low resistivity.

3.5.2 Location maps and cross-sections for Harshaw Creek Dataset

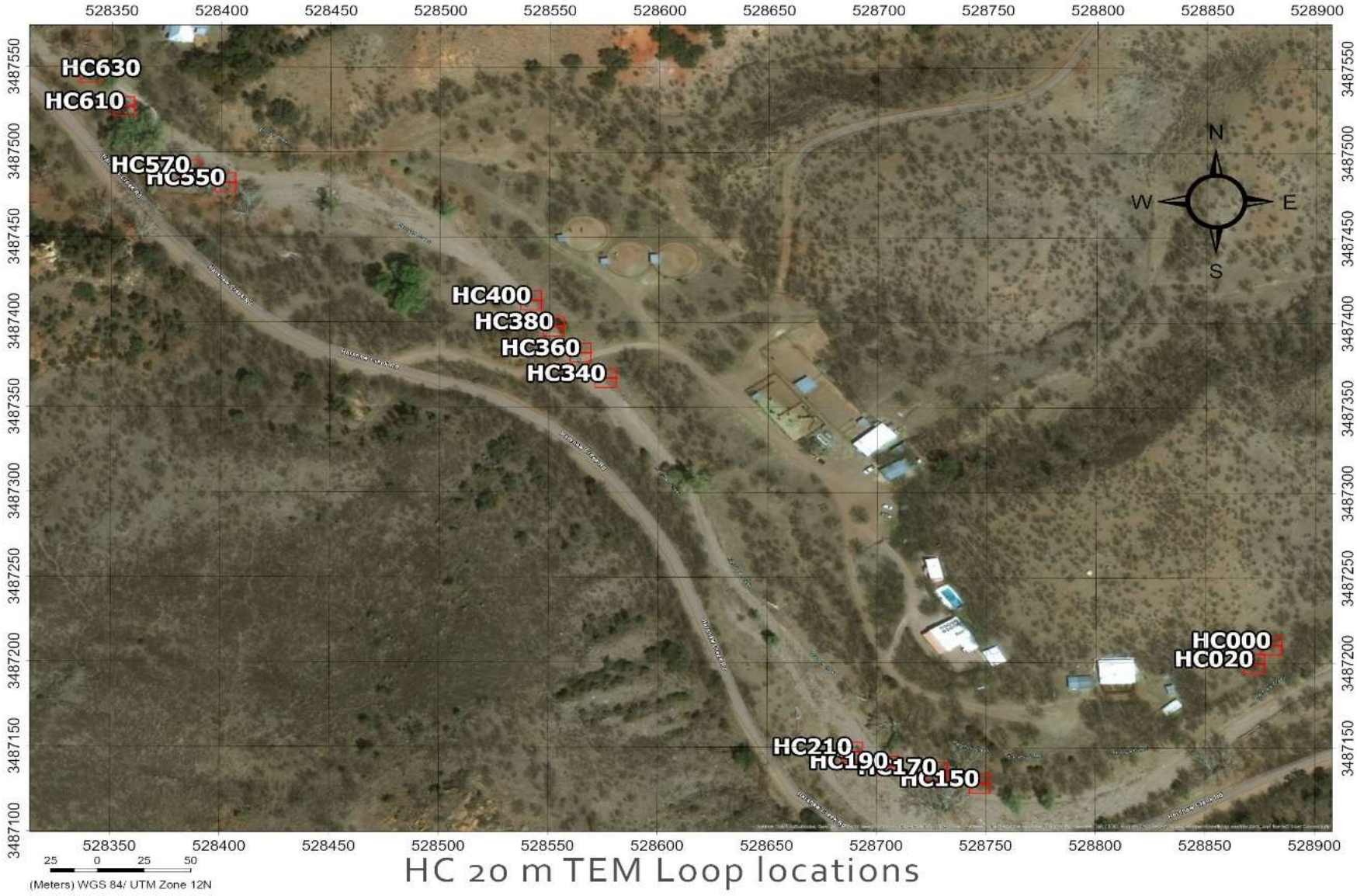

Figure 3.6. Harshaw Creek TEM Location Map with loop Size 20m

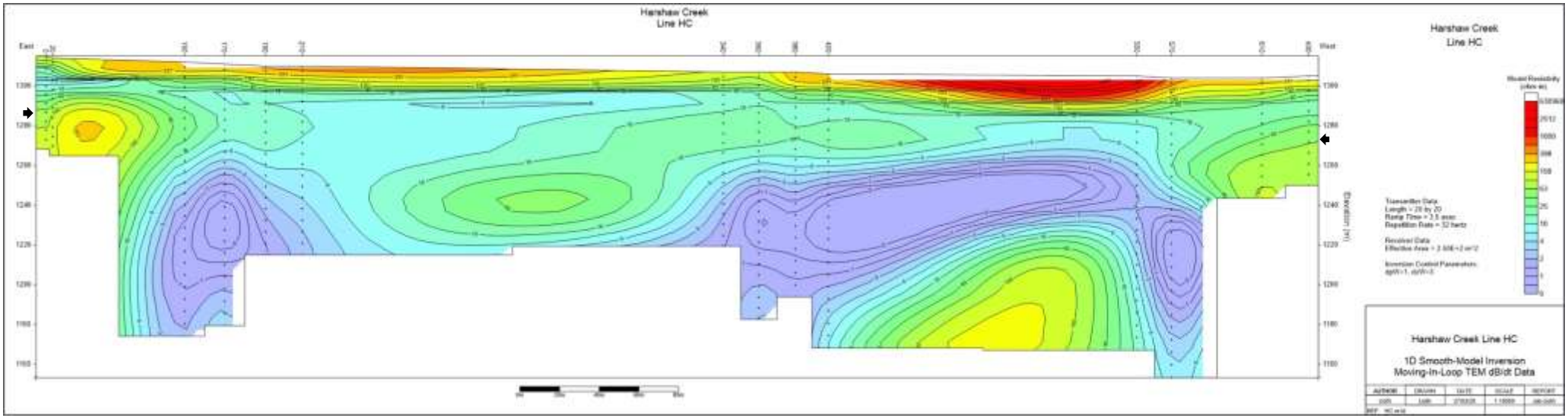

Figure 3.7. Harshaw Creek TEM model with elevation data, 20m loop. Note warm colors indicate high resistivity and cool colors indicate low resistivity.

3.6 Interpretation

For the Red Rock Ranch, there is a distinct boundary between the conductive layer and the resistive layer. As shown in Figure 3.5, the boundaries appear at 17-20m below the surface. That indicates that at this depth range, the water concentration increases, which can indicate the groundwater table is around 17-20m below the surface. The results are similar in Figure 3.7. Based on Figure 3.7 the boundary appears around 15 m, which means that the groundwater table shows up at around 15m below the surface.

Based on Figures 3.5 and 3.7, TEM data cross-sections for Red Rock Ranch and Harshaw Creek, there are some significant anomalies. The first anomalies appear in both Red Rock Ranch and Harshaw Creek. Below a certain depth, the resistivity data are of the order of 0.1 Ohm-m. Based on water-sample conductivity measurements in the area (Floyd Gray, personal communication), it is not feasible to explain these very low resistivities using Archie's Law. A likely explanation for these extremely low resistivities is the presence of a sulfide rich body. The following paper shows a range of resistivities for sulfide rich bodies: Electrical Geophysical Investigations of Massive Sulfide Deposits and Their Host Rocks, West Shasta Copper-Zinc District" Robert J. Horton, Bruce D. Smith and James C. Washburn. The table below (Table 3.1) is reproduced from that paper. The table shows a resistivity range between 0.05-1.4 ohm-m for rocks like massive sulfides.

Rock type	Resistivity ohm-m at 1 Hz range (mean)	Phase mrad at 1 Hz range (mean)	Phase peak	Comments
Massive sulfide	0.05–1.4 (0.5)	10–150 (50's)	Variable	(1)
Altered rhyolite	400–2,000 (100's)	10–40 (30's)	(2)	
Gossan	10–150 (50's)	10–60 (30's)	(3)	Partially saturated
Kennett shale	200–5,000 (1,000's)	20–130	Not well developed	Presumably like siliceous Bragdon Formation and Copley Greenstone
Weathered shale	10,000		High	

(1) Correlation noted between resistivity and phase magnitude
(2) Intermediate frequencies
(3) Intermediate to high frequencies

Table 3.1. West Shasta Electrical Rock Properties (Horton, eta. 1985)

According to Figure 3.5, the TEM data cross-section for Red Rock Ranch shows the surface area has relatively higher resistivity, compared to the deeper area, especially between stations 300-450. Based on our in-field observations, these areas are the riverbed (wash) area, with a low concentration of water during the dry season, due to more rapid drainage. Based on Eq.3.1, the lower water concentration will cause a higher resistivity. As mentioned before, the groundwater table appears around 17-20m below the surface. The purple area indicates a potential sulfide rich body. Compared to the water near the boundary, the resistivity of the water near the faults and the sulfide rich body is higher, which means the water near the faults and the sulfide rich body has lower conductivity.

Based on Figure 3.7, the TEM data cross-section for Harshaw Creek has a similar pattern to Figure 3.5. The resistivity of the surface area is higher than the deep area. That is because the surface region of Harshaw Creek, based on field observations, is similar to Red Rock Ranch. At the surface of Harshaw Creek in the riverbed (wash), most of the soil is sand, which has lower water concentration during the dry season. Based on Archie's Law (Eq.3.1), the lower water concentration will cause higher resistivity.

3.7 Transient Decay Curves

3.7.1 Red Rock Ranch

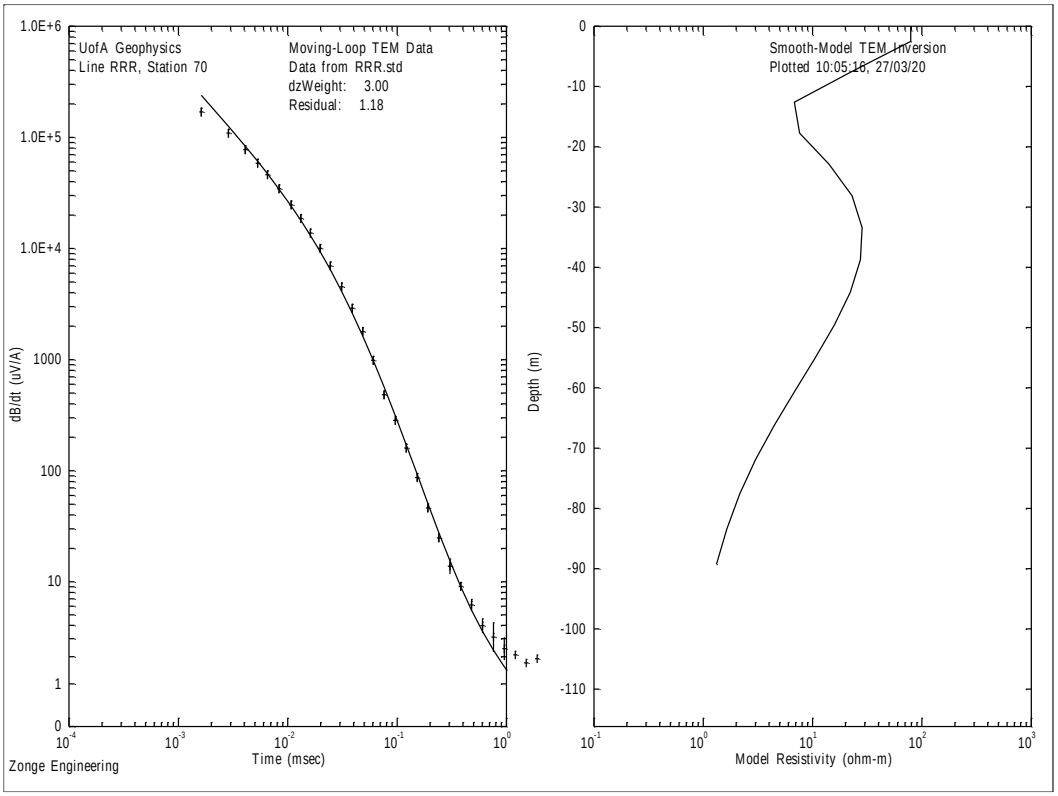

Figure 3.8a. Modeled and Transient Curve for Red Rock Ranch, Station 70, Loop 0001

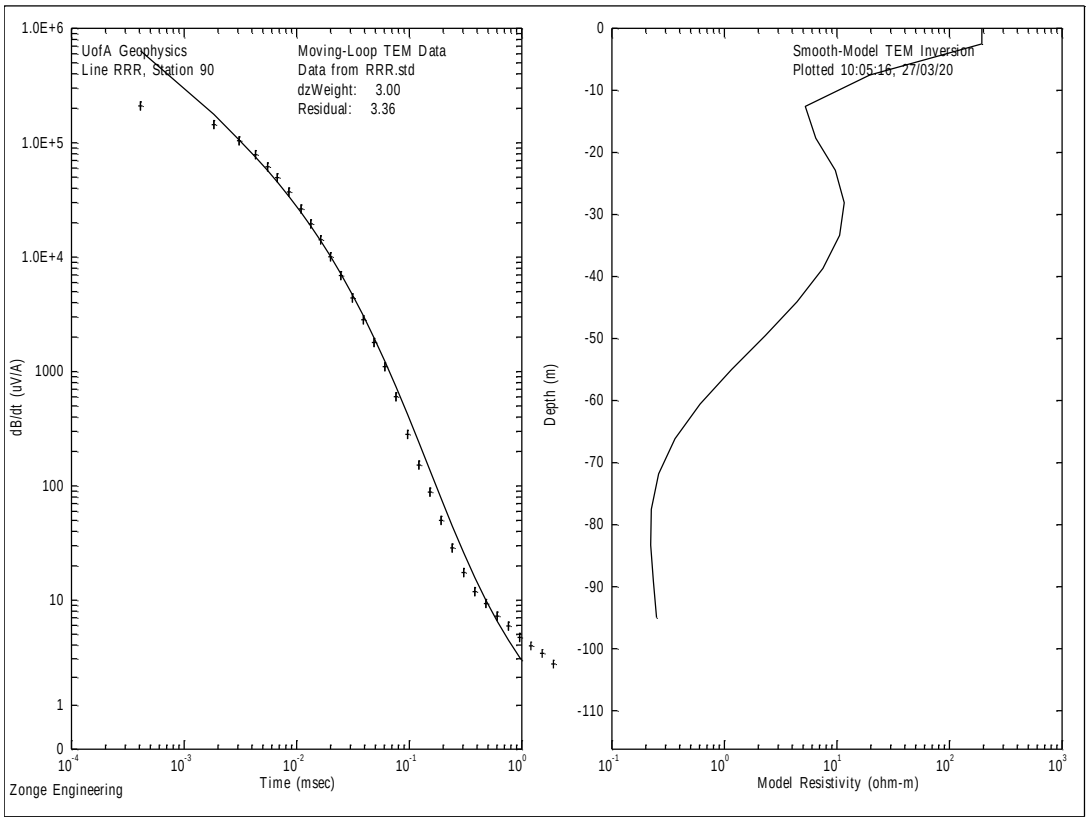

Figure 3.8b. Modeled and Transient Curve for Red Rock Ranch, Station 90, Loop 0002

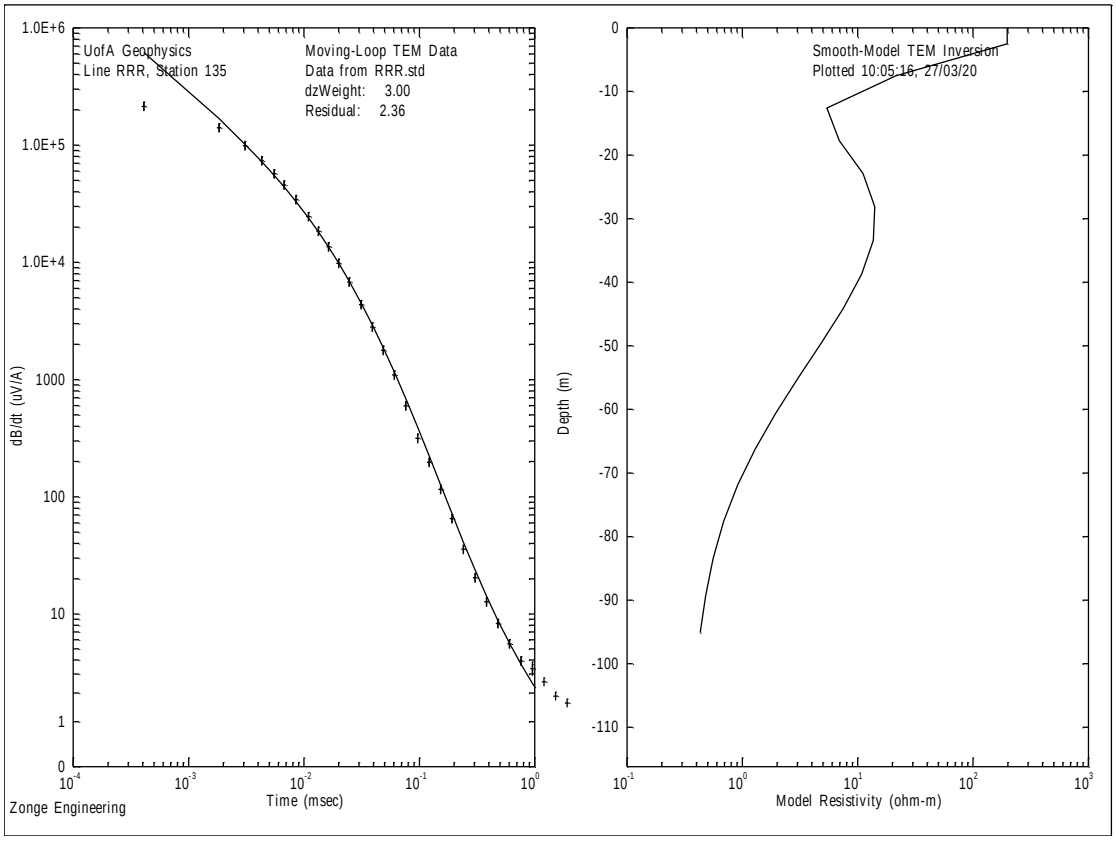

Figure 3.8c. Modeled and Transient Curve for Red Rock Ranch, Station 135, Loop 0003

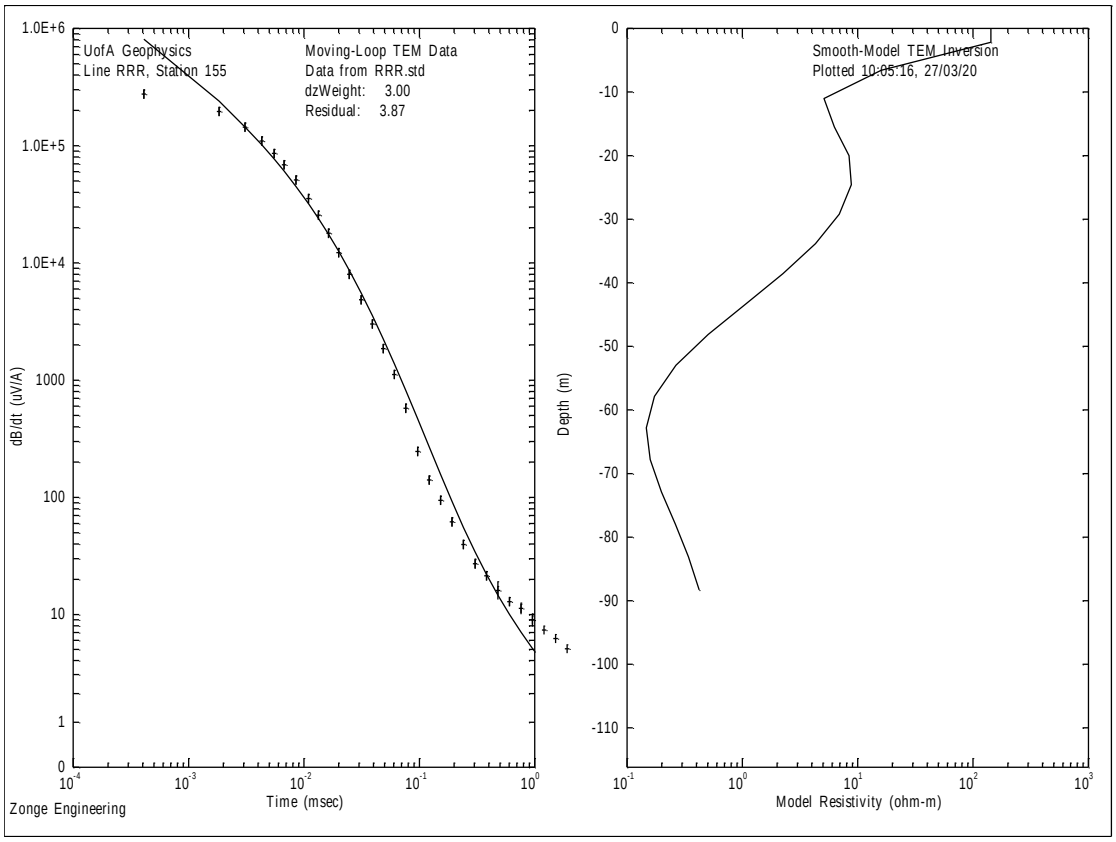

Figure 3.8d. Modeled and Transient Curve for Red Rock Ranch, Station 155, Loop 0004

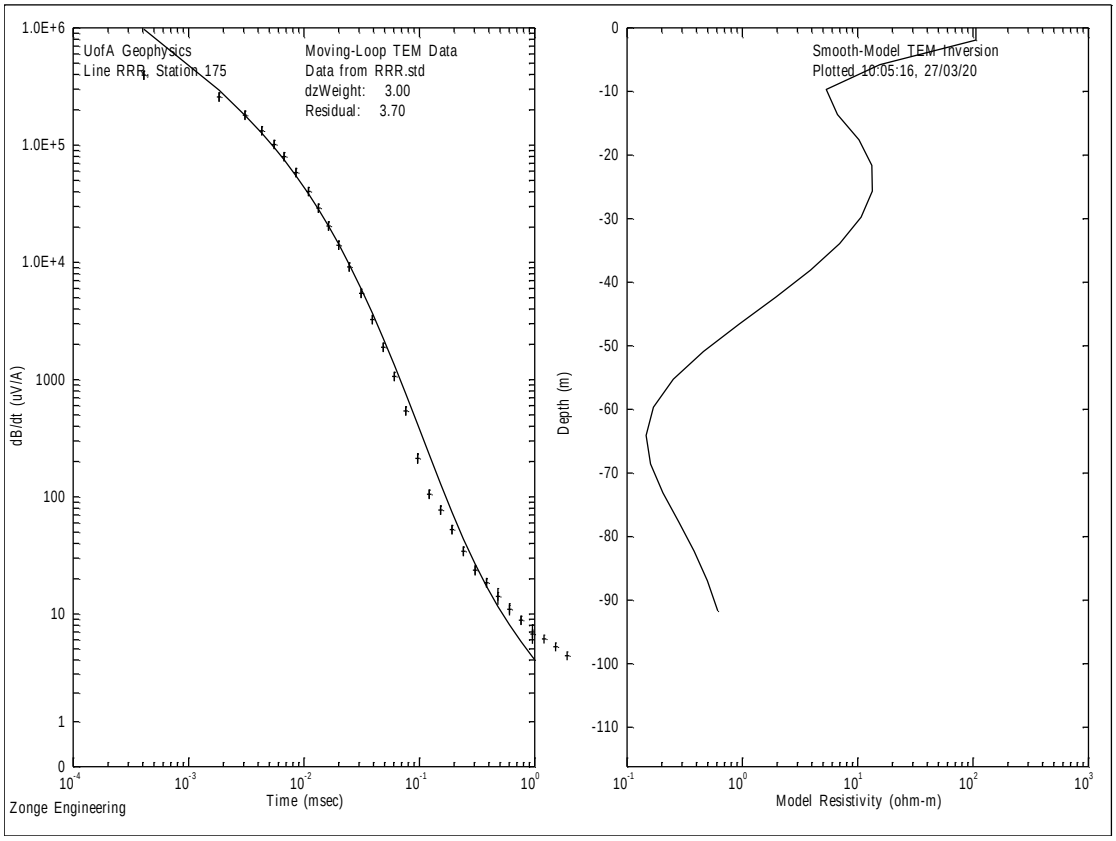

Figure 3.8e. Modeled and Transient Curve for Red Rock Ranch, Station 175, Loop 0005

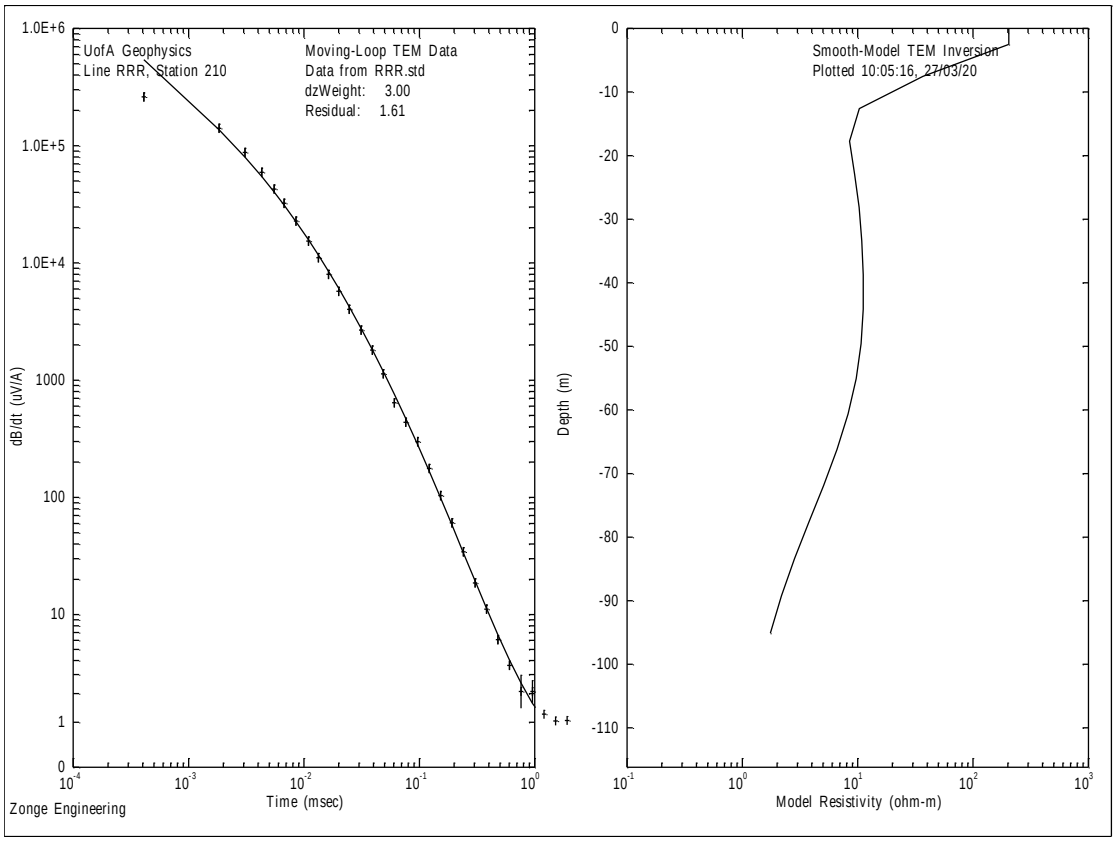

Figure 3.8f. Modeled and Transient Curve for Red Rock Ranch, Station 210, Loop 0006

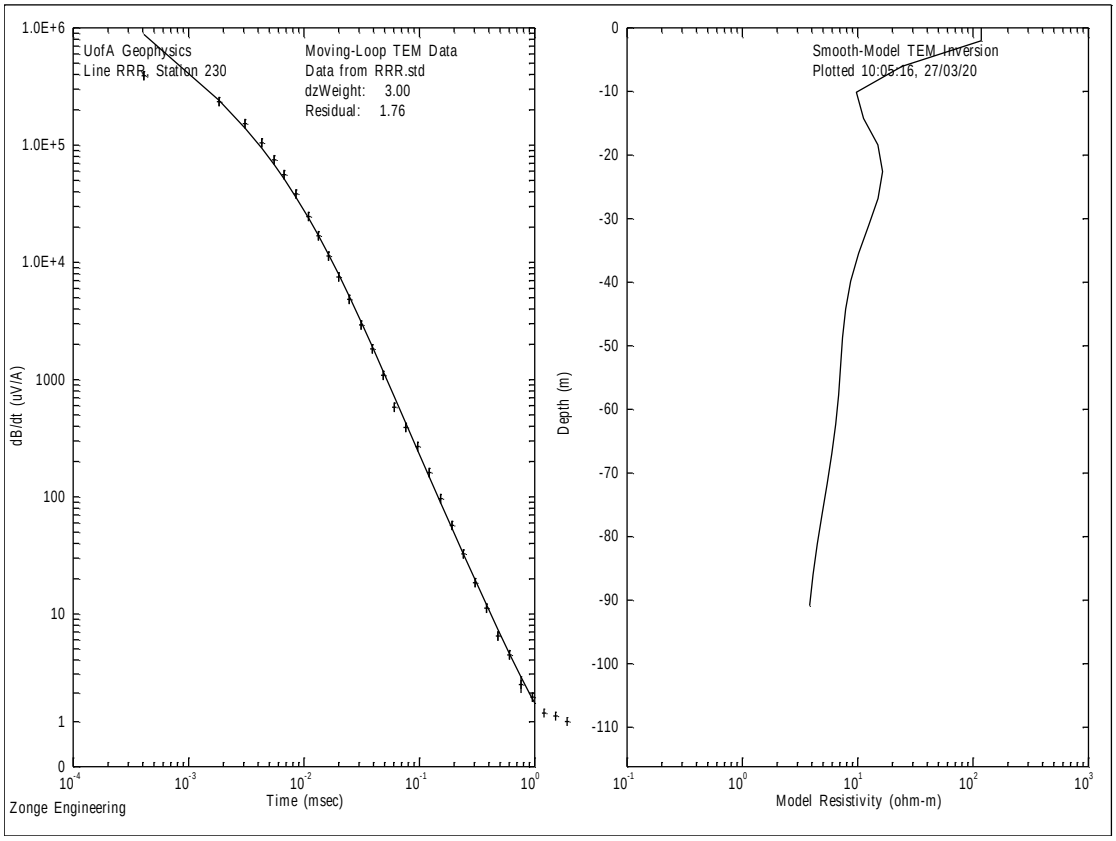

Figure 3.8g. Modeled and Transient Curve for Red Rock Ranch, Station 230, Loop 0007

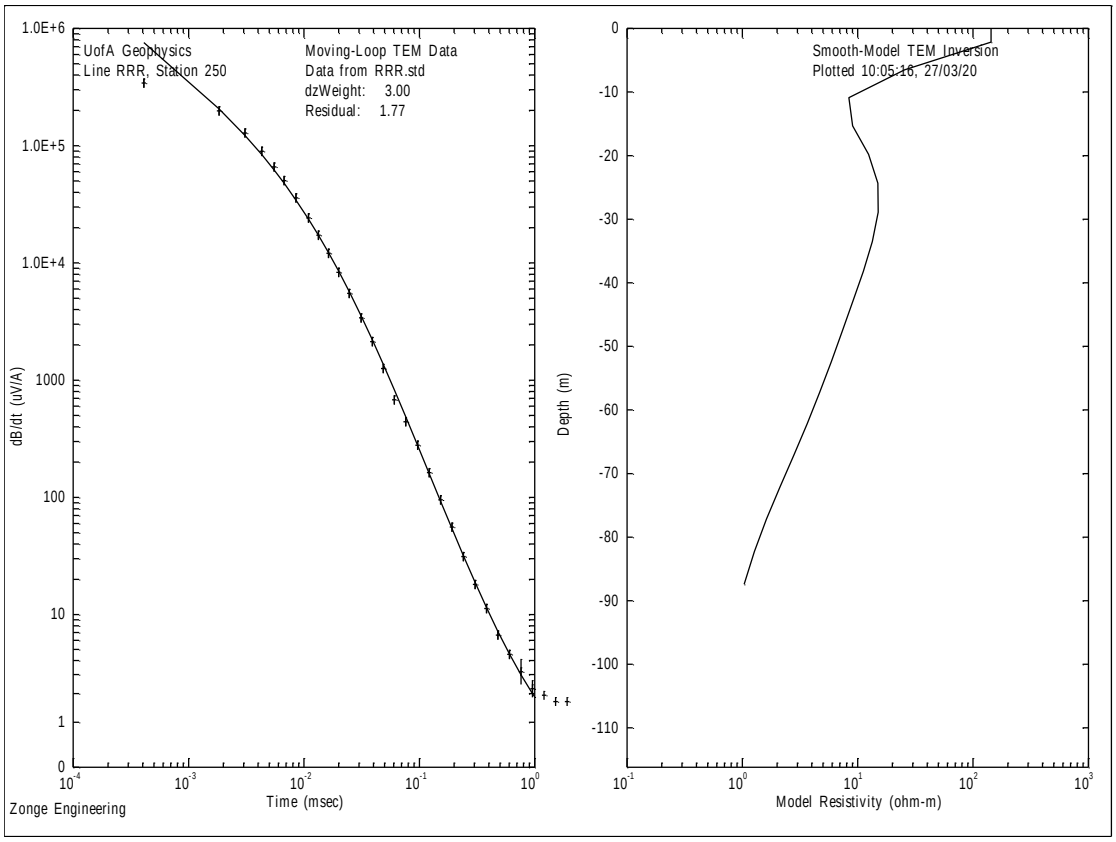

Figure 3.8h. Modeled and Transient Curve for Red Rock Ranch, Station 250, Loop 0008

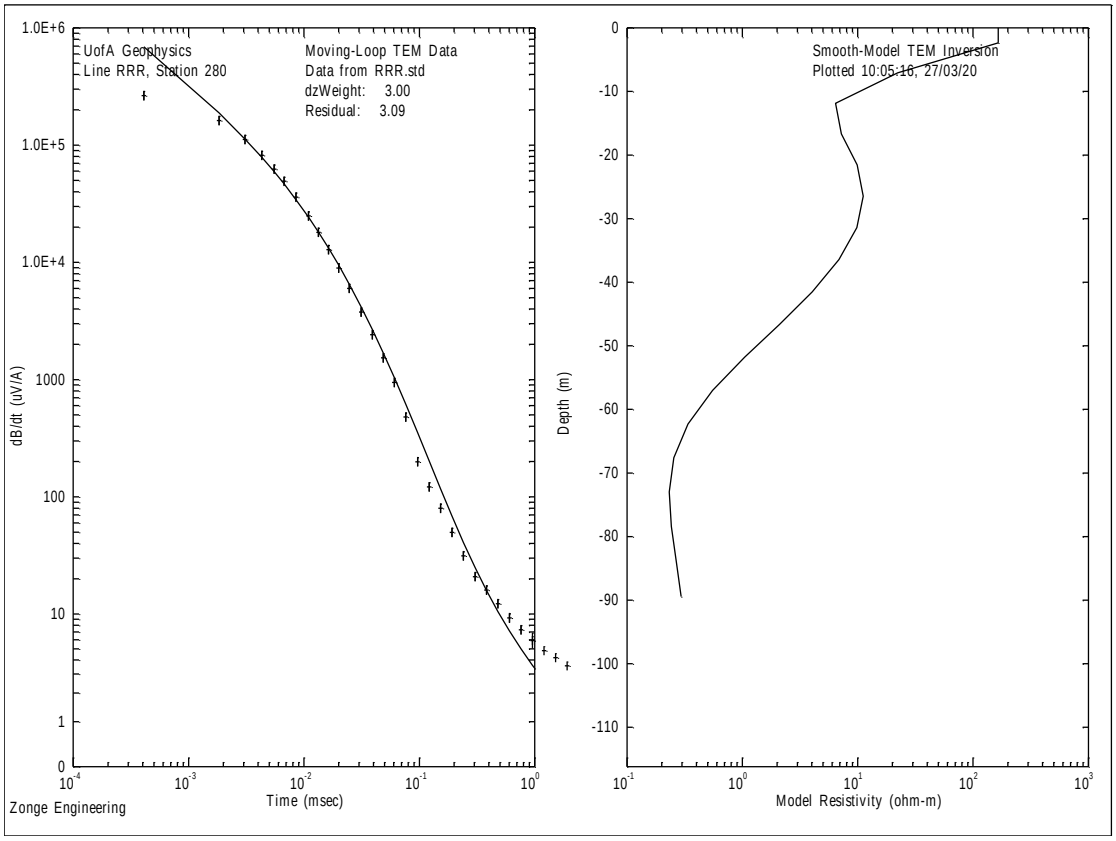

Figure 3.8i. Modeled and Transient Curve for Red Rock Ranch, Station 280, Loop 0009

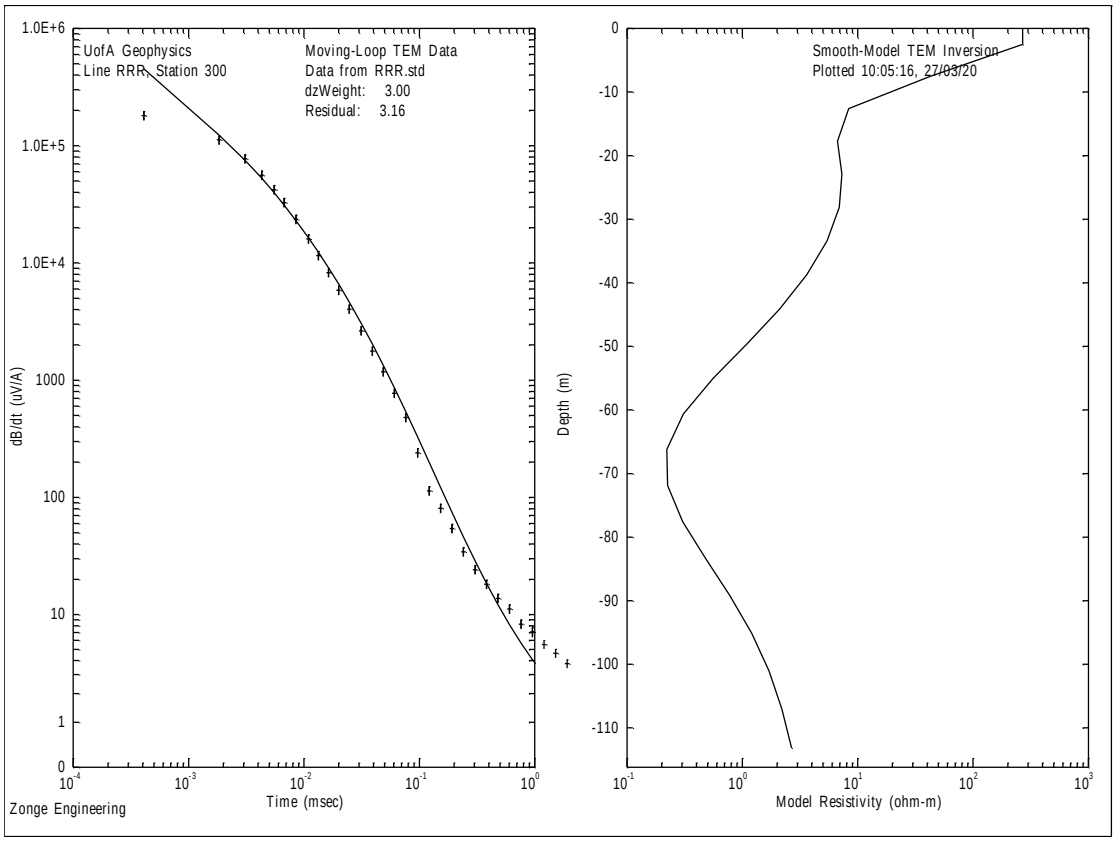

Figure 3.8j. Modeled and Transient Curve for Red Rock Ranch, Station 300, Loop 0010

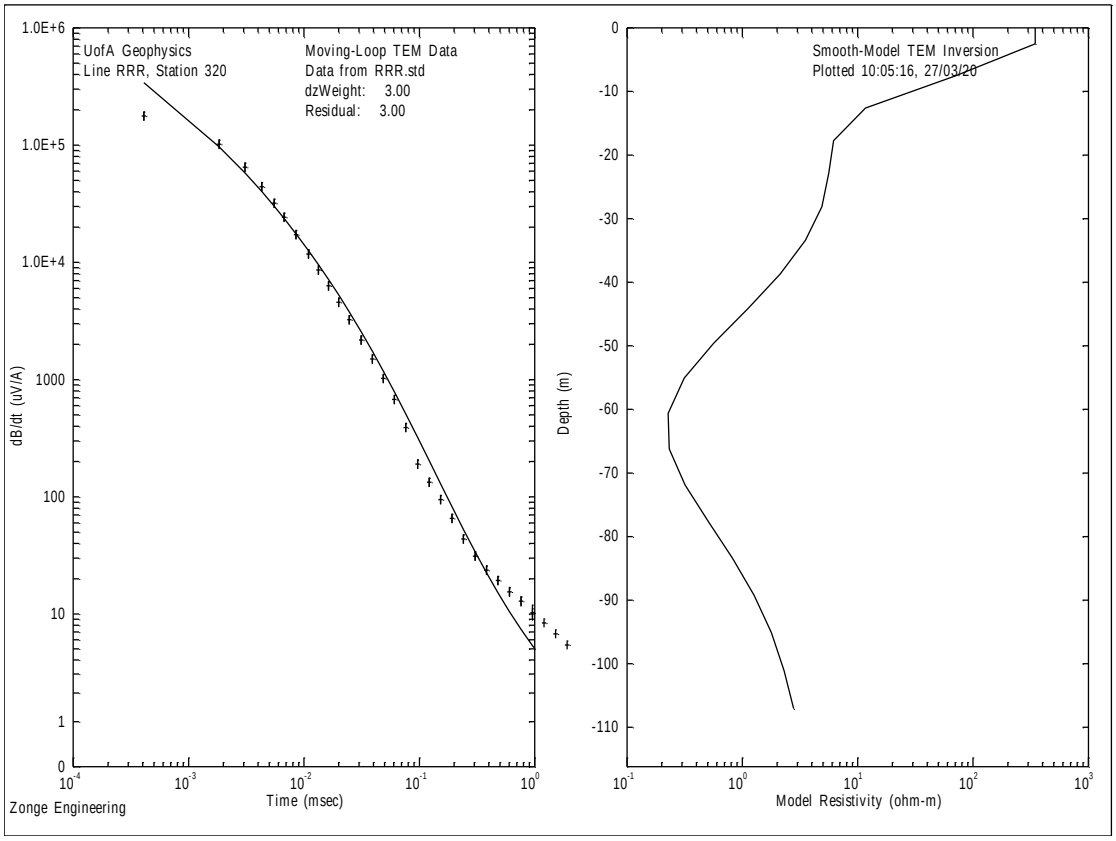

Figure 3.8k. Modeled and Transient Curve for Red Rock Ranch, Station 320, Loop 0011

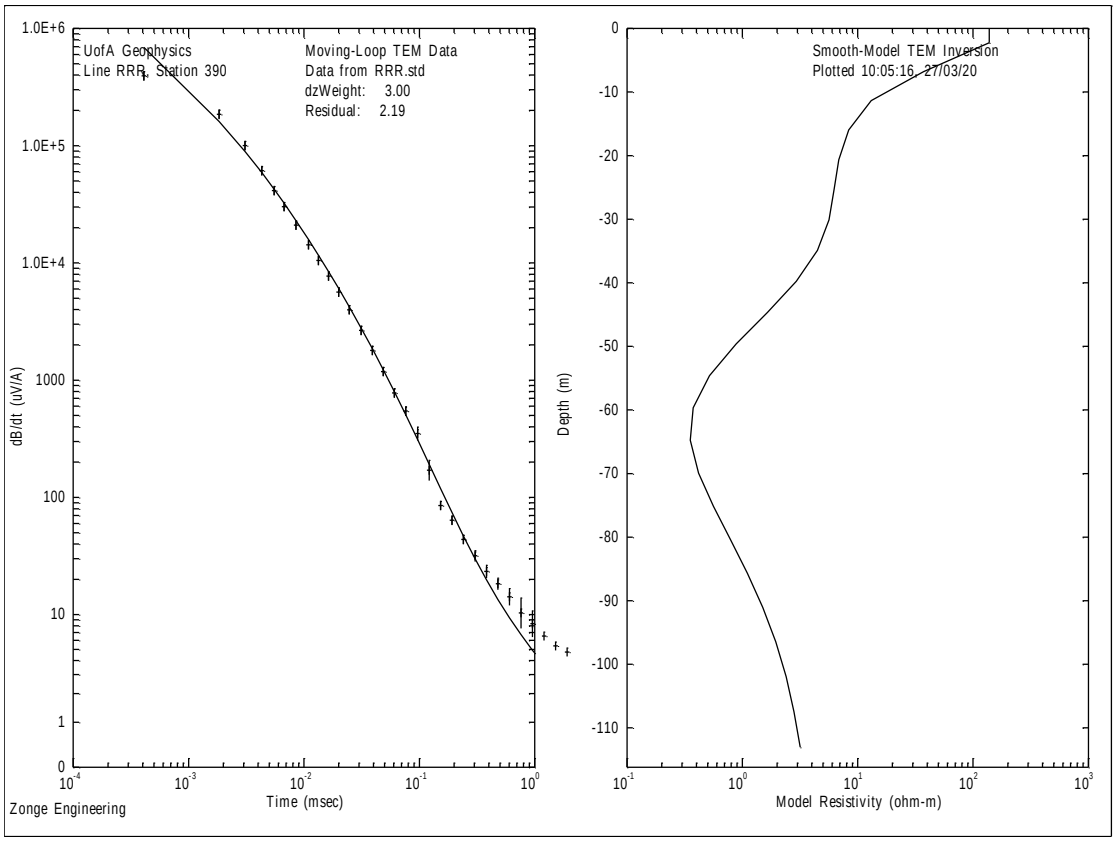

Figure 3.8l. Modeled and Transient Curve for Red Rock Ranch, Station 390, Loop 0012

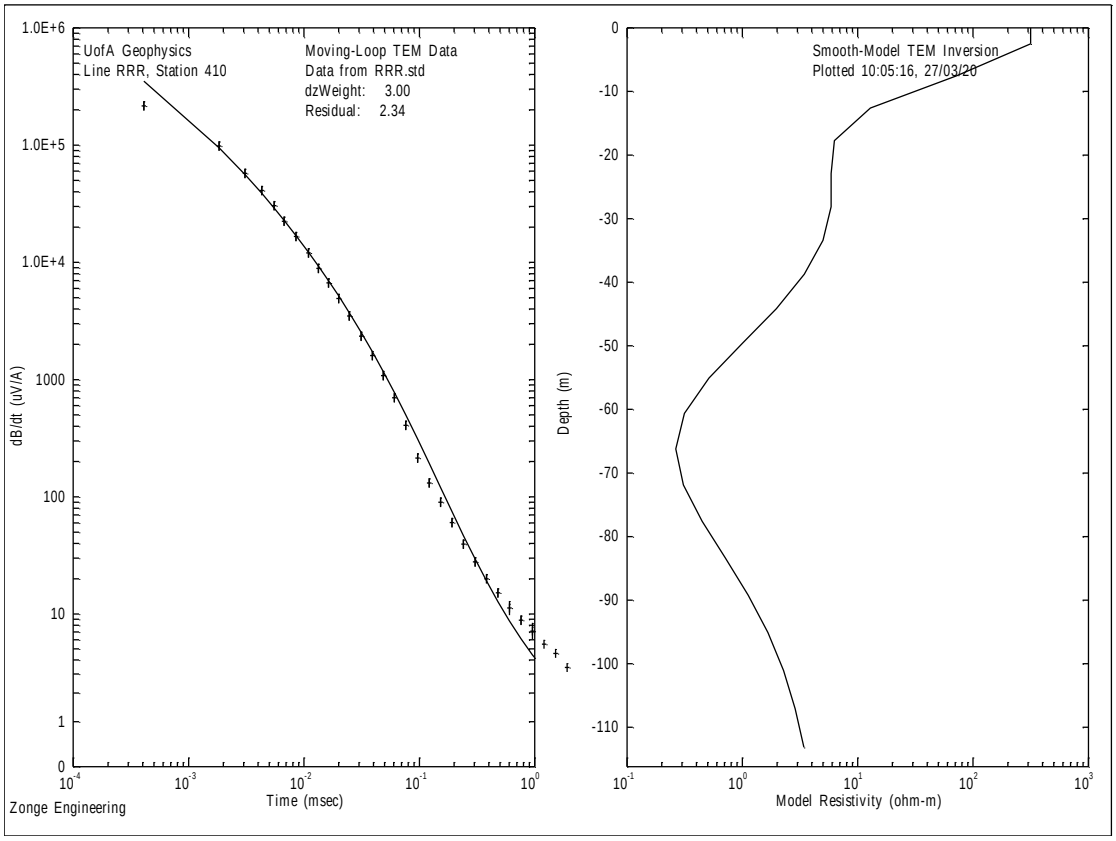

Figure 3.8m. Modeled and Transient Curve for Red Rock Ranch, Station 410, Loop 0013

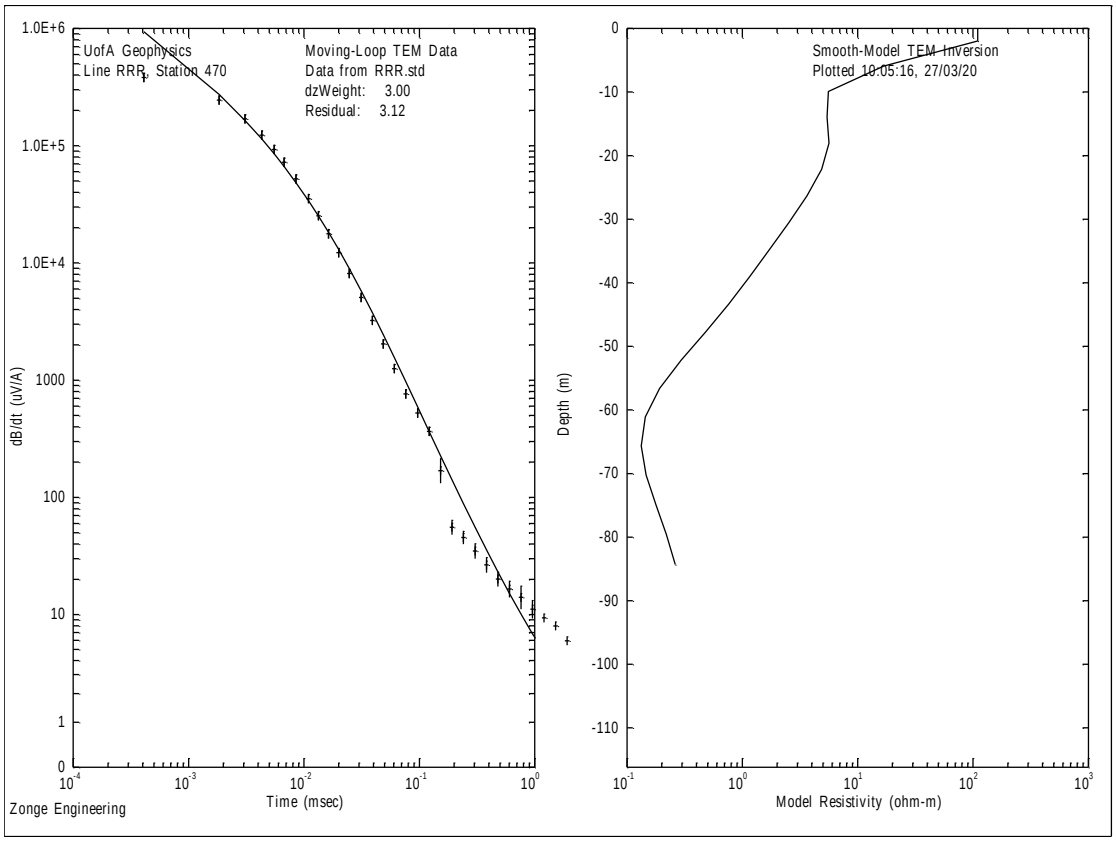

Figure 3.8n. Modeled and Transient Curve for Red Rock Ranch, Station 470, Loop 00014

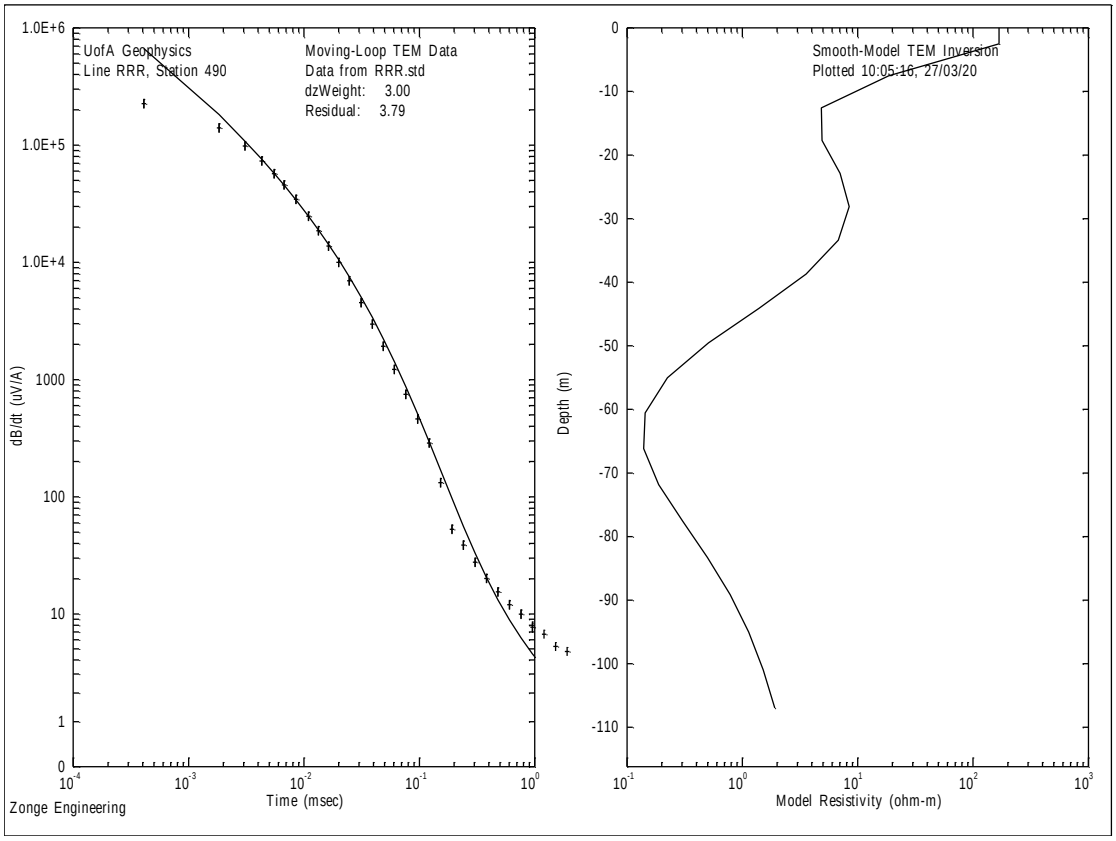

Figure 3.8o. Modeled and Transient Curve for Red Rock Ranch, Station 490, Loop 0015

3.7.2 Harshaw Creek

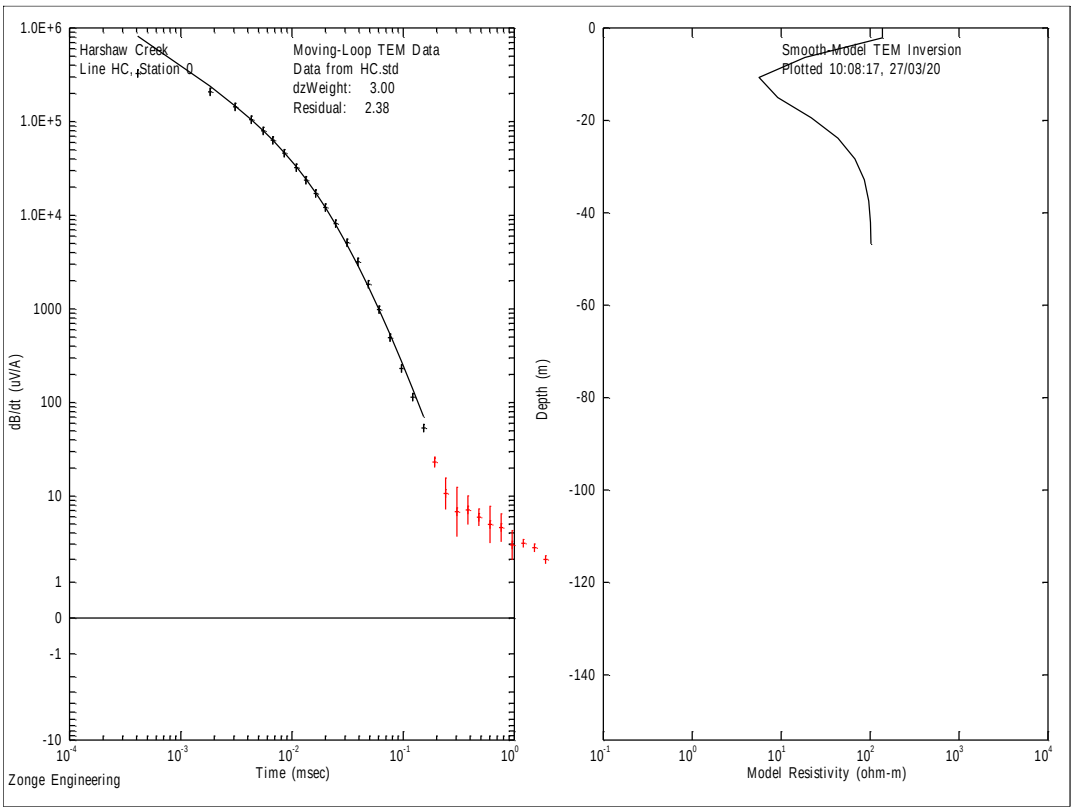

Figure 3.9a. Modeled and Transient Curve for Harshaw Creek, Station 0, Loop 0001

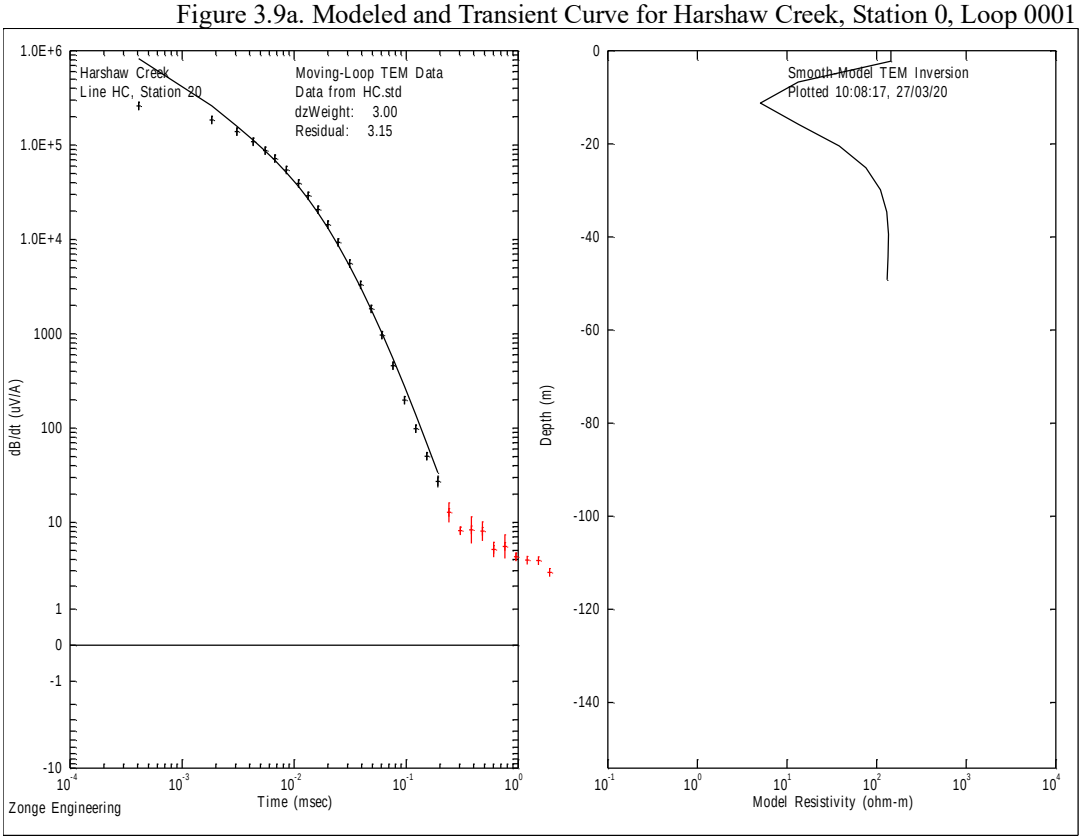

Figure 3.9b. Modeled and Transient Curve for Harshaw Creek, Station 20, Loop 0002

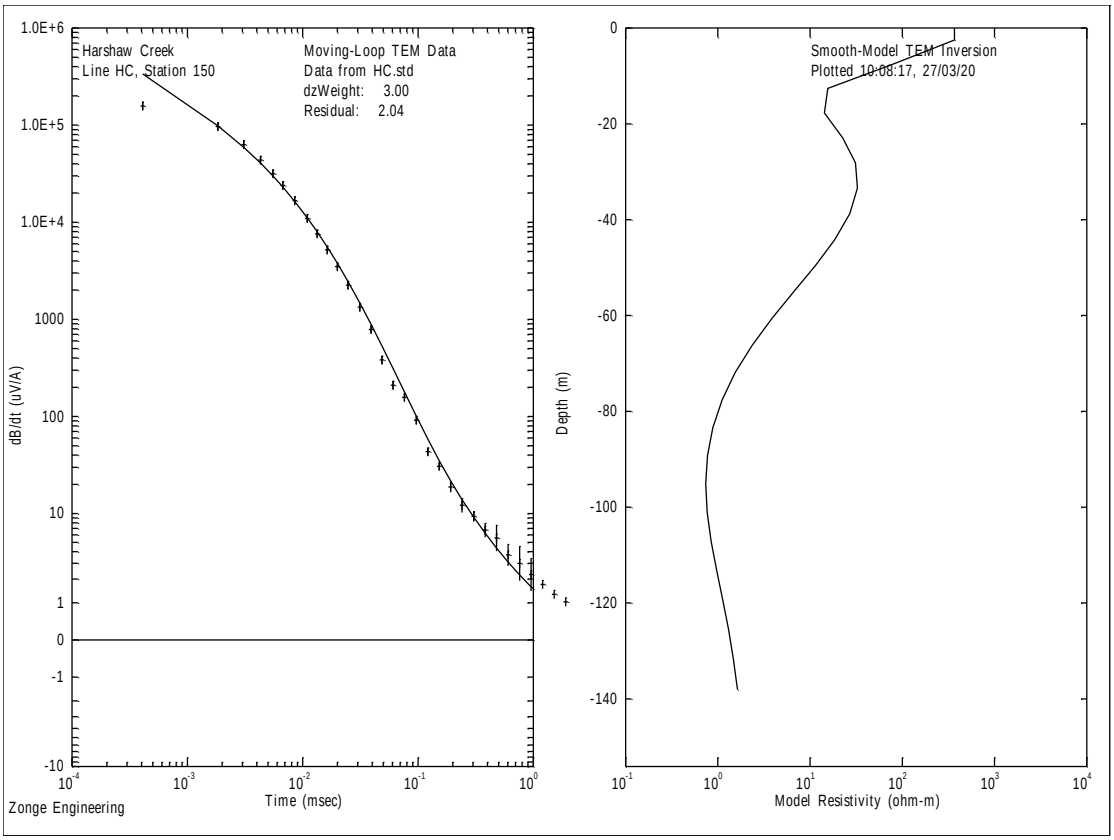

Figure 3.9c. Modeled and Transient Curve for Harshaw Creek, Station 150, Loop 0003

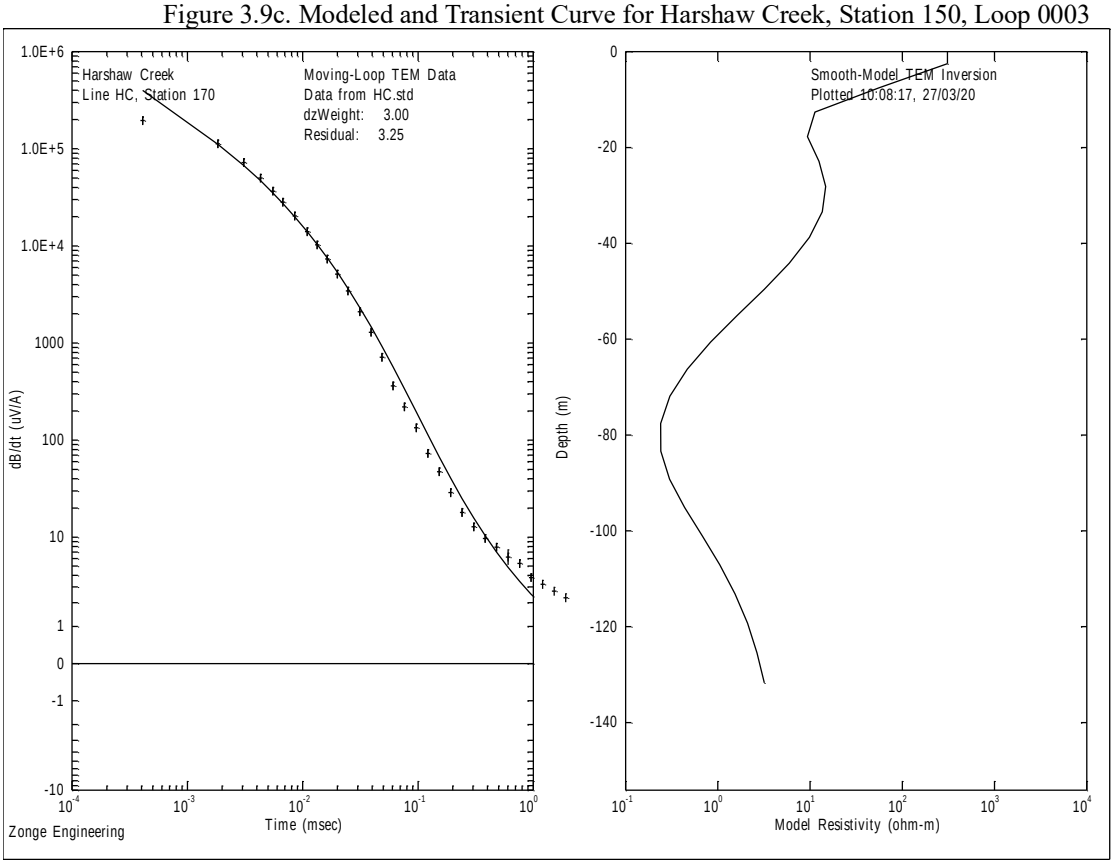

Figure 3.9d. Modeled and Transient Curve for Harshaw Creek, Station 170, Loop 0004

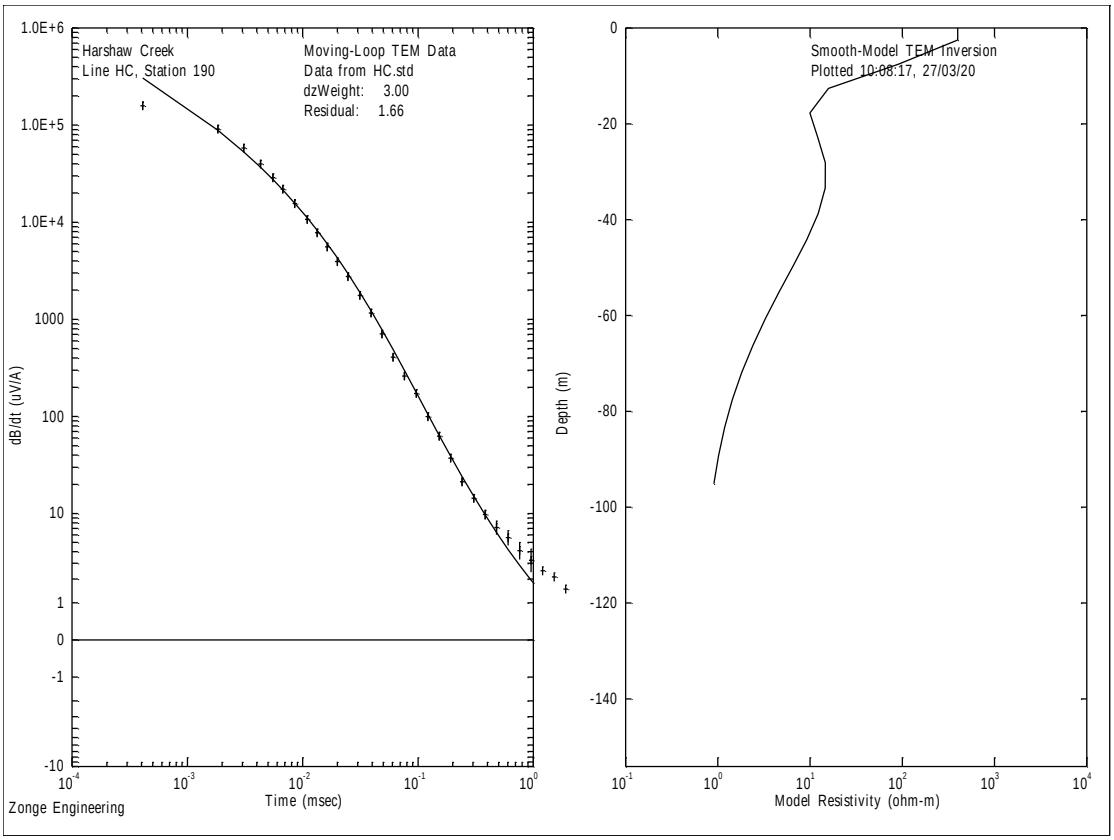

Figure 3.9e. Modeled and Transient Curve for Harshaw Creek, Station 190, Loop 0005

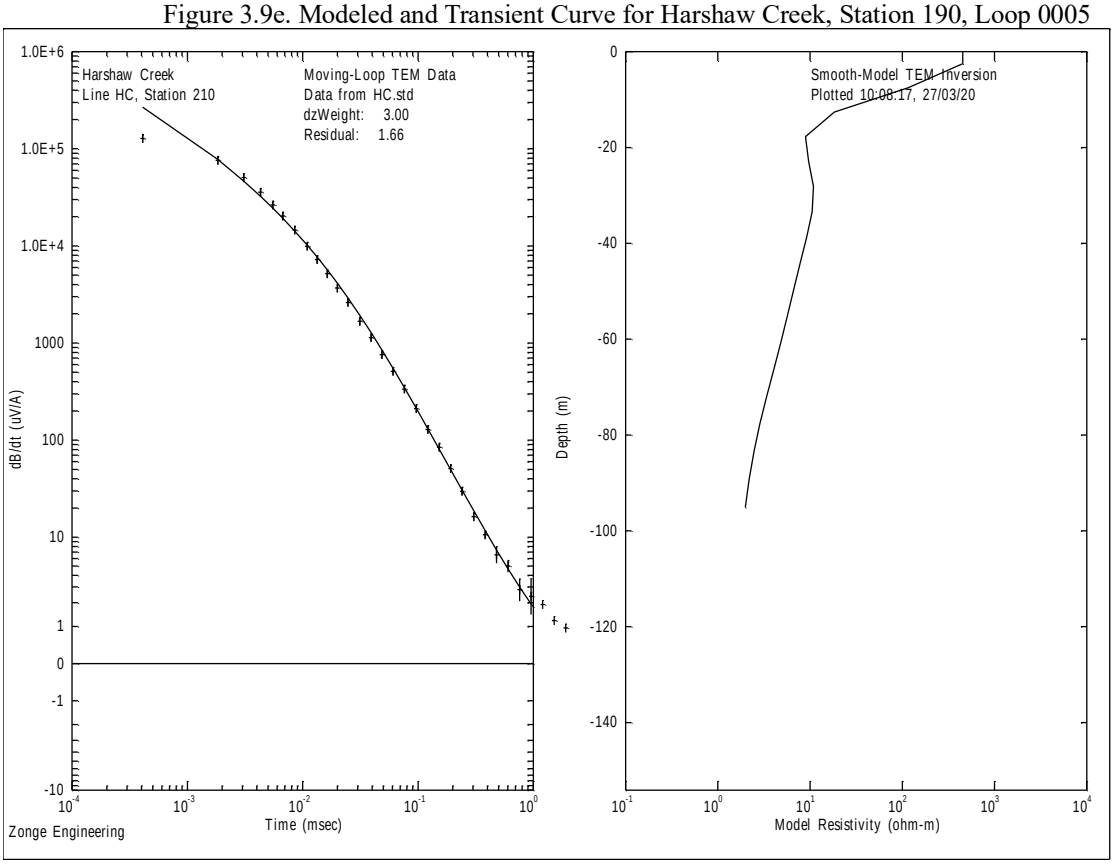

Figure 3.9f. Modeled and Transient Curve for Harshaw Creek, Station 210, Loop 0006

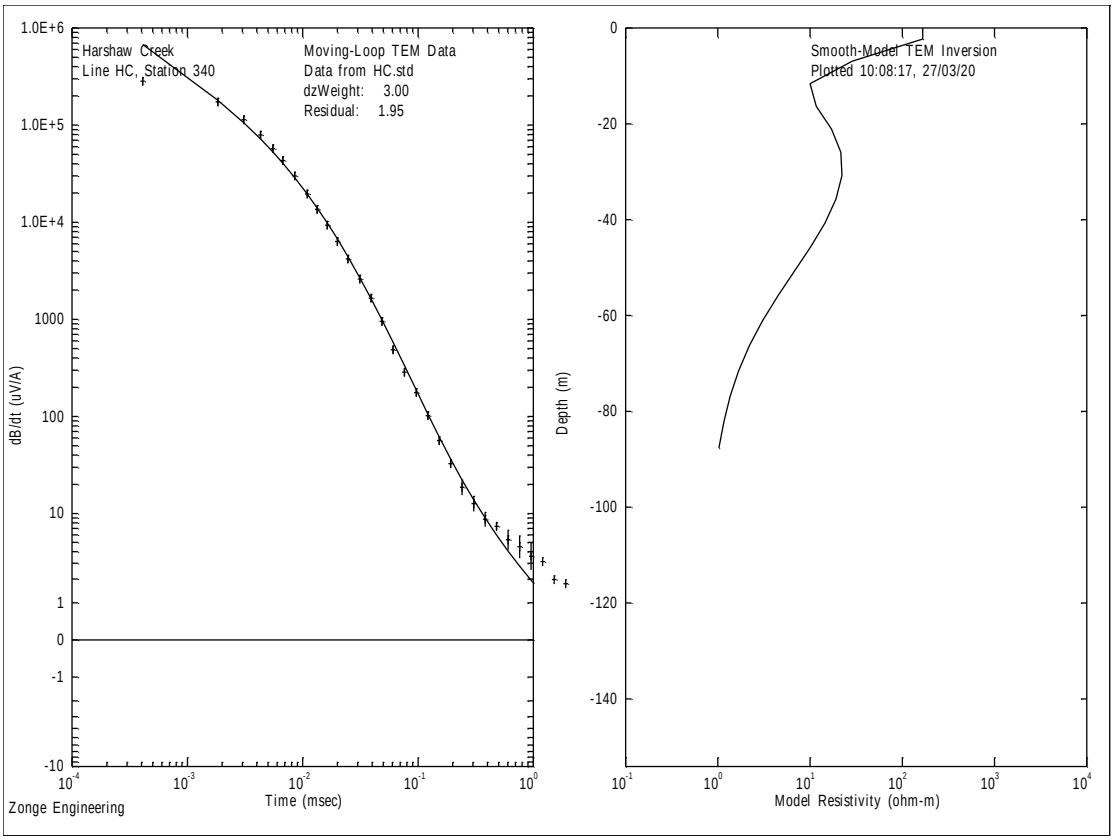

Figure 3.9g. Modeled and Transient Curve for Harshaw Creek, Station 340, Loop 0007

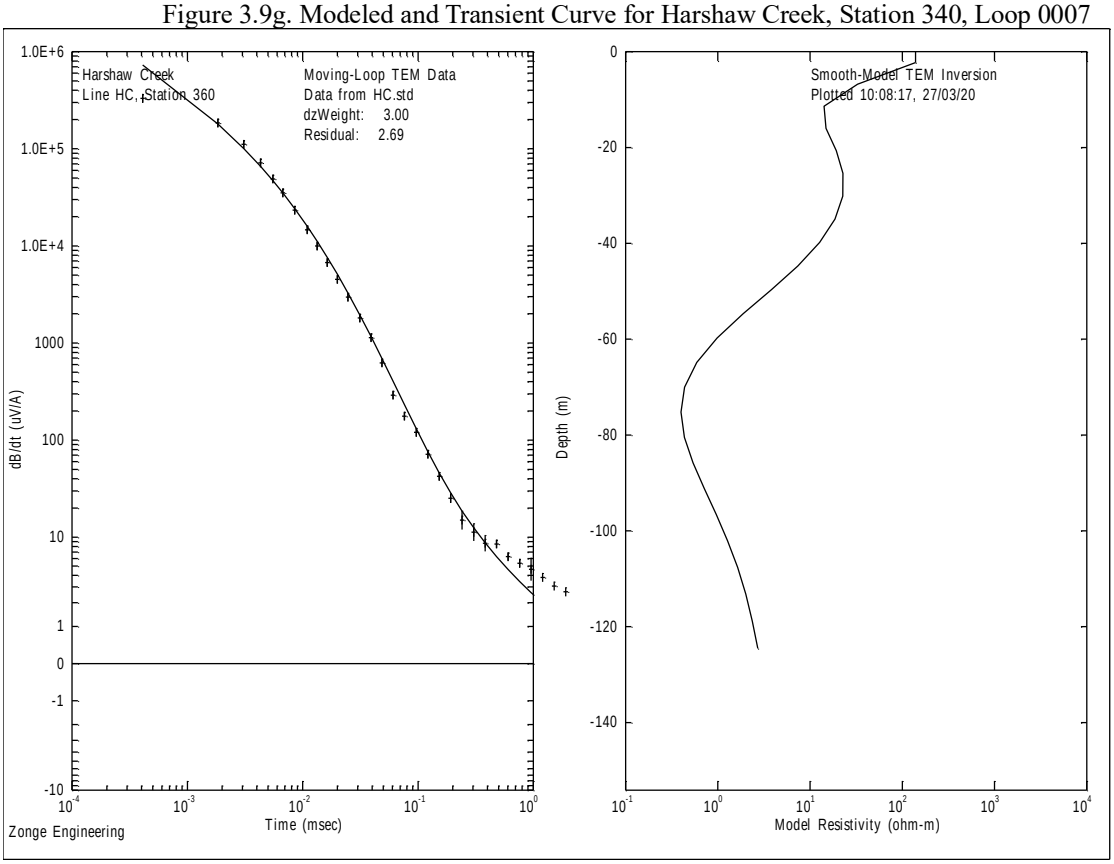

Figure 3.9h. Modeled and Transient Curve for Harshaw Creek, Station 360, Loop 0008

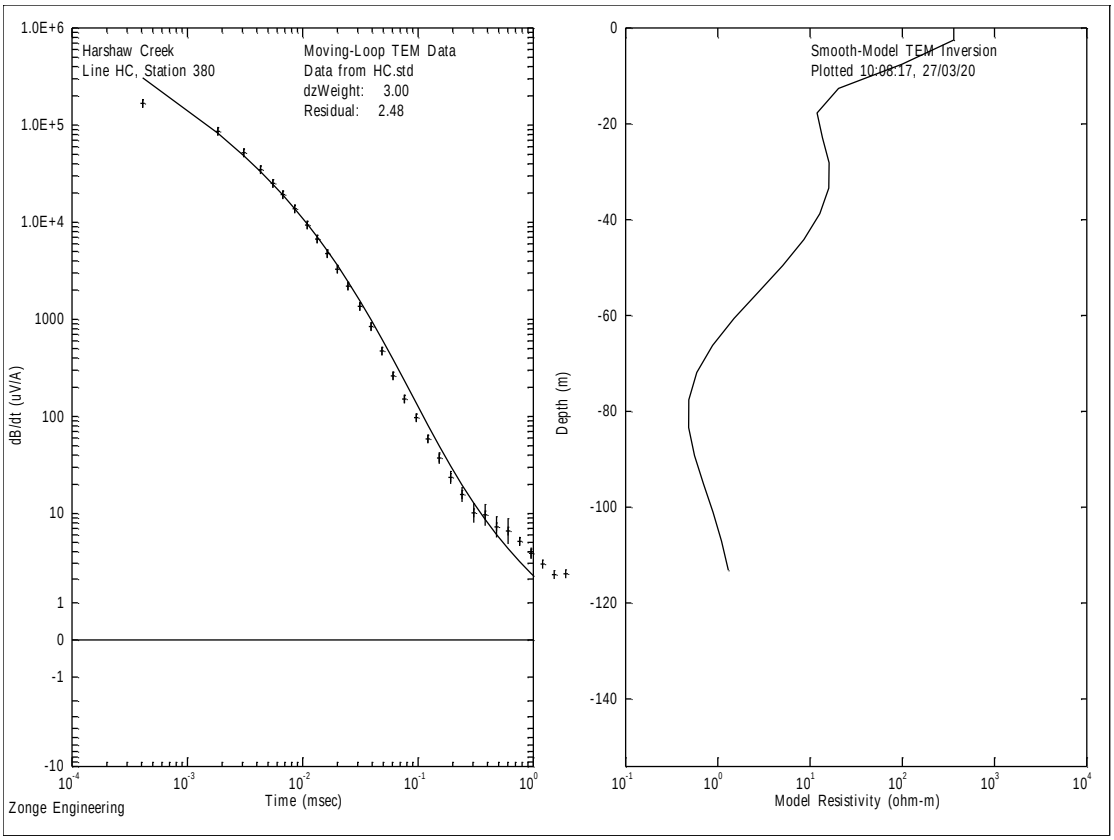

Figure 3.9i. Modeled and Transient Curve for Harshaw Creek, Station 380, Loop 0009

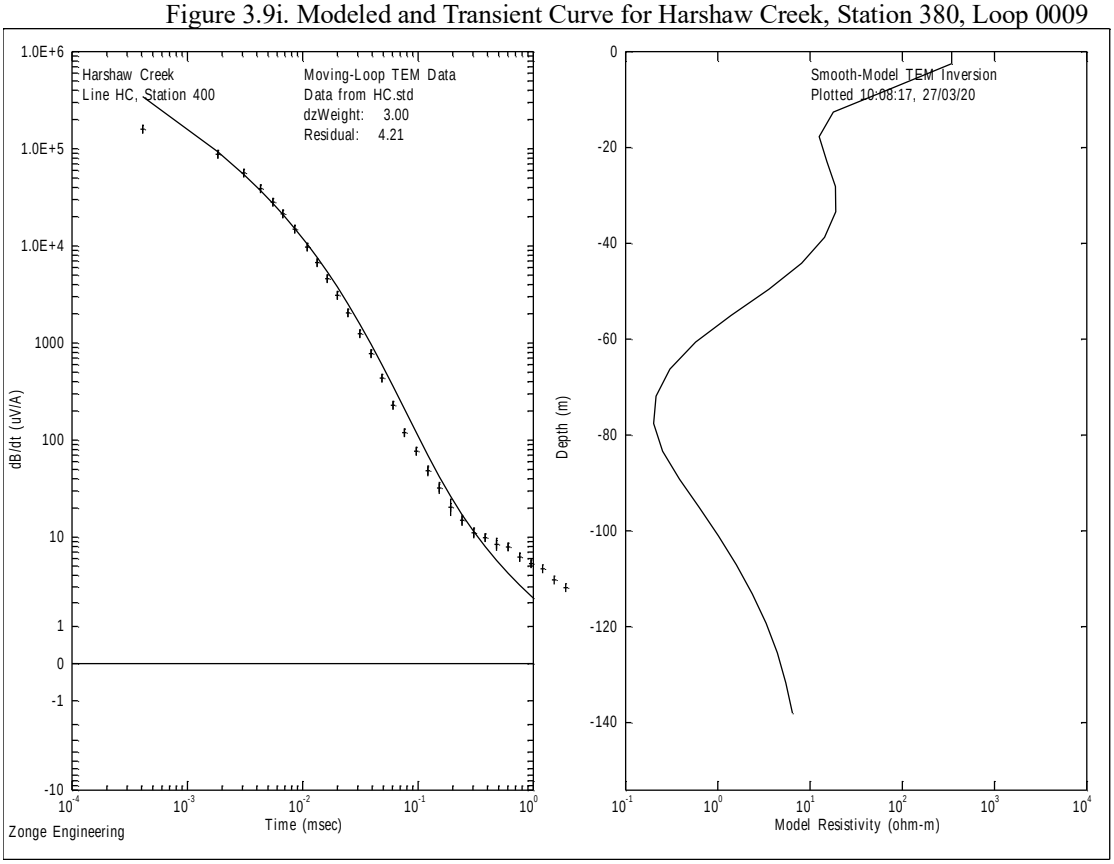

Figure 3.9j. Modeled and Transient Curve for Harshaw Creek, Station 400, Loop 0010

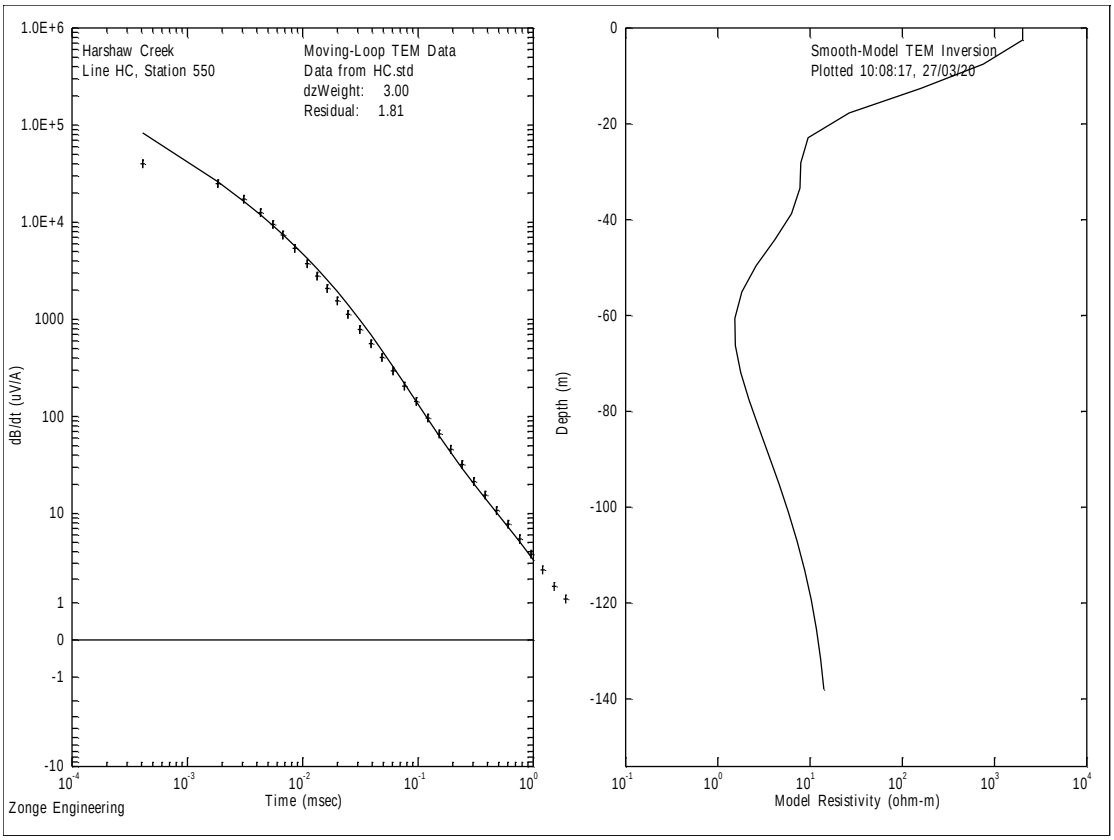

Figure 3.9k. Modeled and Transient Curve for Harshaw Creek, Station 550, Loop 0011

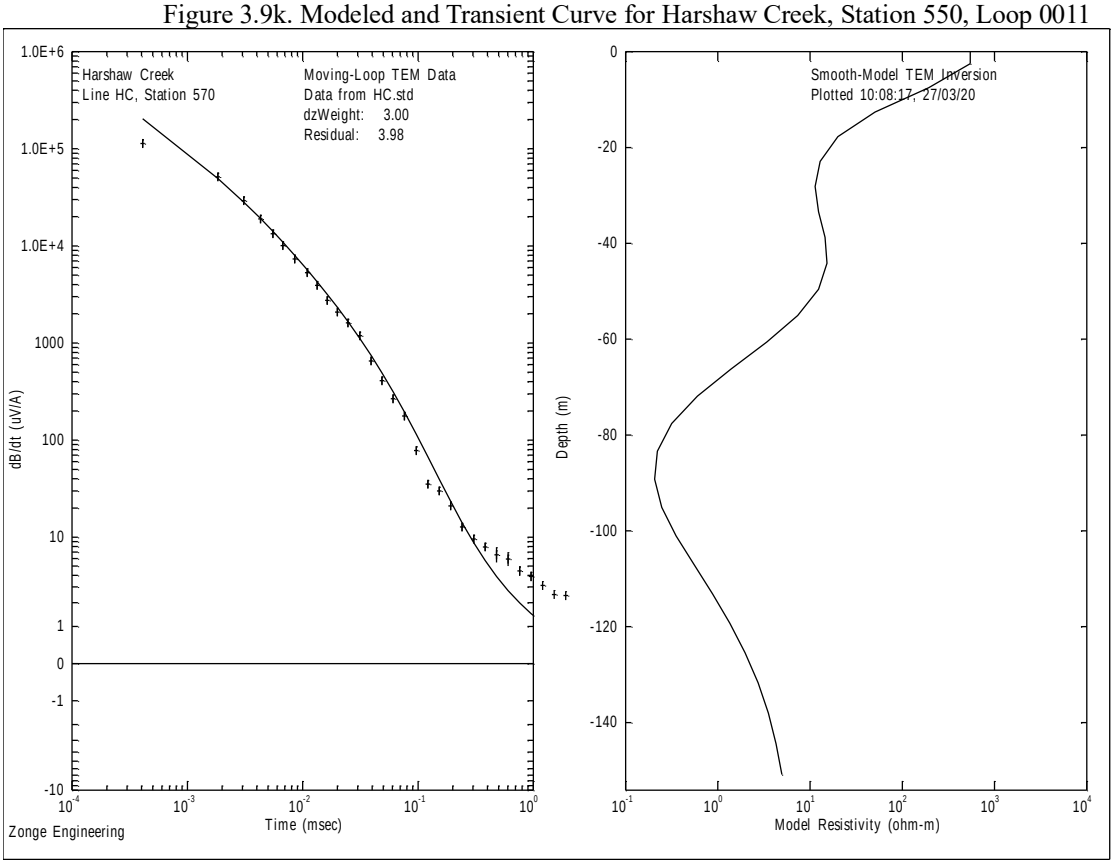

Figure 3.9l. Modeled and Transient Curve for Harshaw Creek, Station 570, Loop 0012

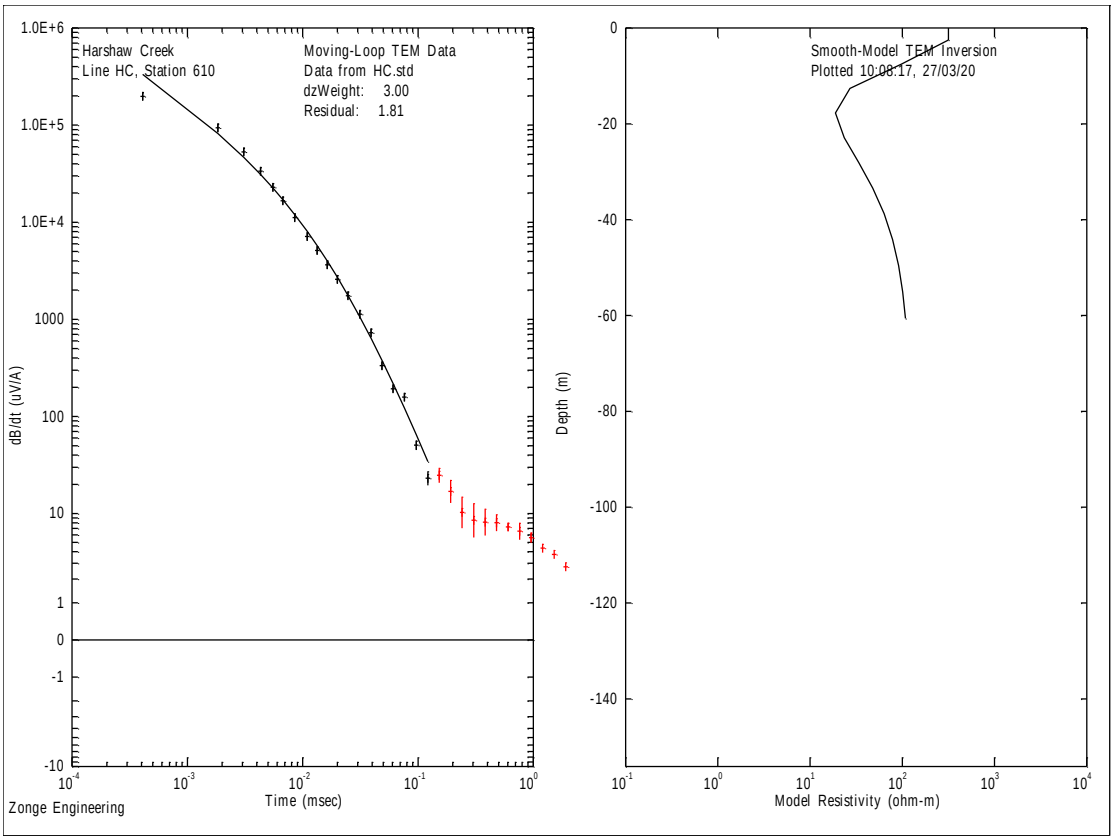

Figure 3.9m. Modeled and Transient Curve for Harshaw Creek, Station 610, Loop 0013

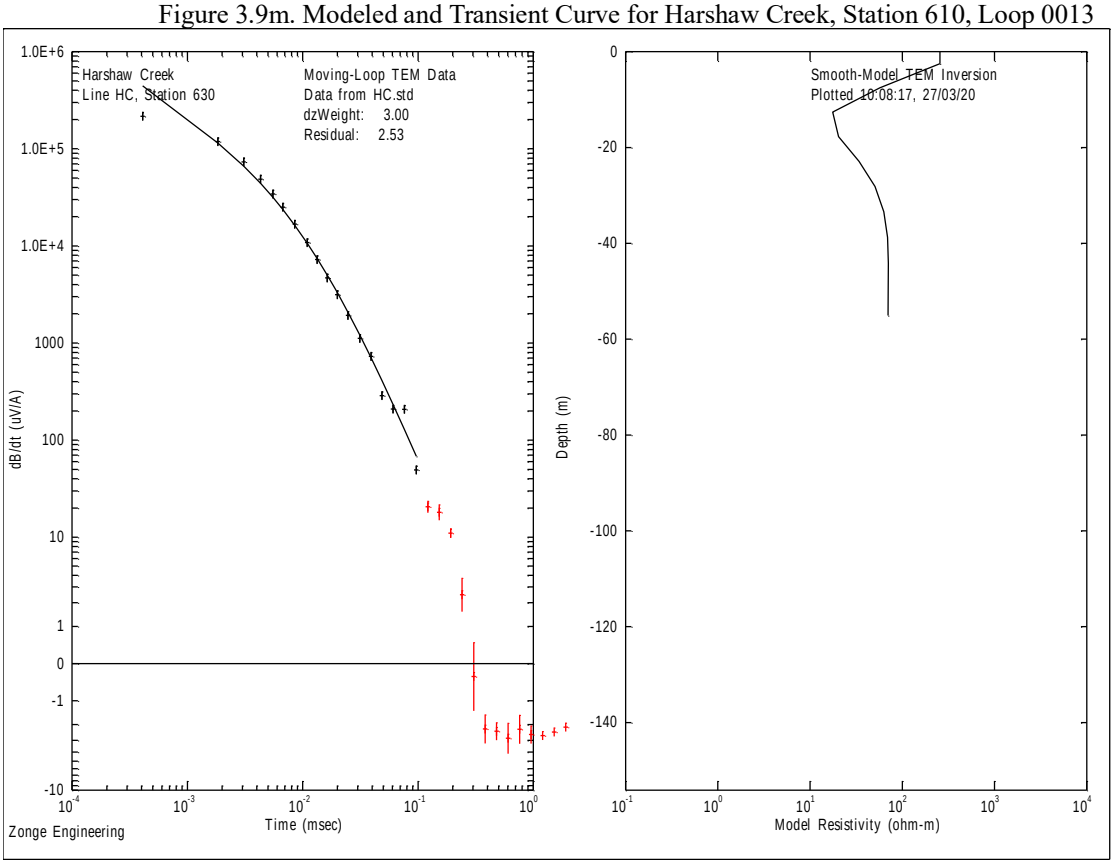

Figure 3.9n. Modeled and Transient Curve for Harshaw Creek, Station 630, Loop 0014

3.8 References

Zonge International, 2020, Transient Electromagnetic of Time-Domain EM (TEM), http://zonge.com/geophysical-methods/electrical-em/tem/, accessed April, 2020.

Reynolds, John, 2011, An Introduction to Applied and Environmental Geophysics: John Wiley and Sons, 292 p.

Robert J.H., Bruce D.S., James C.W., 1985, Electrical Geophysical Investigations of Massive Sulfide Deposits and Their Host Rocks, West Shasta Copper-Zinc District, Economic Geology, pp. 2213-2229

4. DC Resistivity Surveys

4.1 Introduction

This geophysical survey uses the four-terminal method for dipole-dipole and strong gradient (incorporating both Schlumberger and Wenner arrays) direct current (DC) electrode arrays to explore and map resistivity variations in the subsurface. The system utilizes the basic physical principals presented by Ohm's Law, stating that the electric potential (V) is equal to the current (I) multiplied by the total resistance (R). The dipole-dipole array is established such that two pairs of electrodes: a transmitter and a receiver, each with a constant cathode/anode separation distance (a), are planted shallowly into the ground at a distance from each other that is a multiple of the cathode/anode separation (n*a). One pair of electrodes inputs a current into the ground from the surface and the other records the change in electric potential. Raw resistance values may be calculated by dividing the change in potential by the established current (Advanced Geosciences Inc., 2017). The Schlumberger array works in a similar manner, except it places the voltmeter within a wider spaced ammeter. The distance between the anode and cathode attached to the voltmeter is separated by distance (a) and for the ammeter distance (n*a). The Wenner array is used for vertical electrical sounding (VES) in which four evenly spaced electrodes read subsurface resistivity by sending current through the outer two electrodes to be read by the two inner potential electrodes.

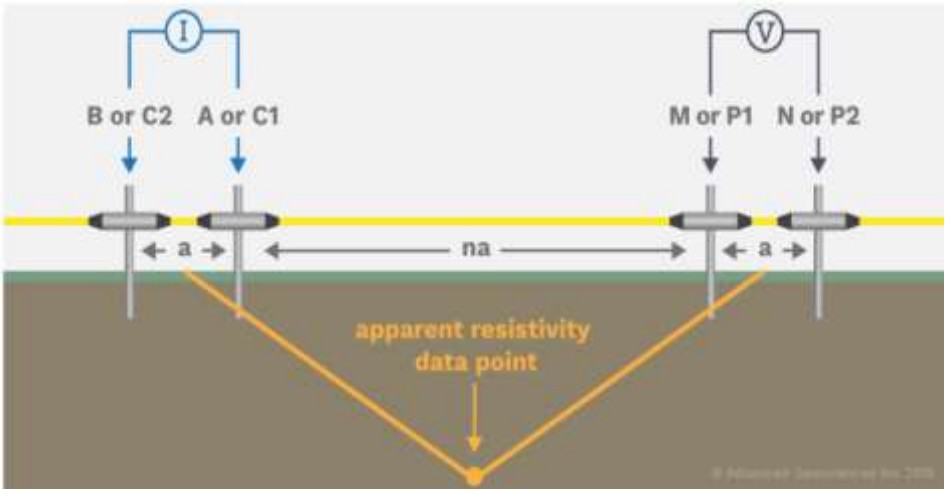

Figure 4.1 A diagram displaying the two oppositely-charged electrode pairs used to determine apparent resistivity (ρ_a) at a given point. The transmitter pair is on the left and sends out current (I). The receiver pair is on the right and reads the change in potential (V). Retrieved from Advanced Geosciences Inc. (2017).

Resistivity is what is being directly measured in the experiment. A solid's resistivity (ρ), given by

$$\rho = \delta R^{*}(\delta A / \delta L), \quad (4.1)$$

is a resistance value that depends on the ratio between the cross-sectional area (A) and the length (L) of the solid material. The relationship between resistance and resistivity is directly proportional. Any time resistivity values are measured in the heterogenous, anisotropic conditions of the whole Earth, they are the apparent resistivity (ρ_a), as they do not reflect the real physical property. A weighted average of these apparent resistivity data is taken to convert observational measurements into data that estimates true resistivities of subsurface layers as given below:

$$\rho_a = (V / I)\ \pi\ a\ n\ (n+1)\ (n+2), \quad (4.2)$$

where (V/I) is the impedance in Ohms, (a) is the separation distance between electrodes, and (n) is the number of spacings (a) between each dipole (Wightman et al., 2016).

The resistivity of zones in the Earth varies based on the natural electrical conductivity of a material, its structure (i.e. porosity, degree of fracture), and level of saturation. Dry rock of common mineral composition tends to resist electrical transmission and act as an insulator. However, the electrical conductivity of water is high in comparison and groundwater contains other dissolved compounds and particulate solids that assist the flow of electrons. Water saturates subsurface layers by invading permeable unconsolidated or fractured units and occupying the open pore space and/or fault interface channels. Therefore, electrical resistivity of a rock unit is inversely proportional to its porosity and saturation, as given by Archie's Law:

$$\rho = \frac{a\rho_w}{\phi^m S_w^n}, \quad (4.3)$$

where ρ is the observed resistivity, ρw is the resistivity of water, Φ is the fractional porosity, Sw is the fractional water saturation, and the tortuosity factor, a, the cementation exponent, m, and the saturation exponent, n are empirical constants with typical values of 1, 2, and 2 respectively.

4.2 Field Procedures and Instrumentation

Two separate four-terminal DC dipole-dipole array surveys were conducted at the site along Harshaw Creek near Red Rock Ranch outside of Patagonia, Arizona. The main array survey lines are conglomerations of a series of smaller surveys, each composed of 56 stainless steel rod electrodes planted shallowly into the topsoil with five meters of spacing and connected by a series of multiconductor cables. These survey conglomerations are referred to as roll-along surveys. Conductivity of the electrodes was assisted by the artificial saturation of the contact interface with highly saline water.

For each roll-along segment, the data collection system, the AGI SuperSting R8 resistivity meter in combination with the AGI Swift switch box, is centered in the middle of the 56-electrode array. The SuperSting, on its eight separate channels, automatically manages and changes the transmitter/receiver configurations along the line of electrodes, reading data relative to the midpoint between the dipole pairs, to produce the best resolution resistivity cross-section along the transect from the surface to maximum reliable depth. After each array is surveyed, the front half of the electrode array remains in place while the trailing half is "rolled-along" to the leading end (i.e. the center of the next array) to continue the transect line with overlapping data records between arrays.

Figure 4.2 This image displays the correct operational setup using the SuperSting resistivity meter, Swift switch box, and 12V battery connected to the multiconductor cables and steel electrodes. Photo retreived from Advanced Geosciences Inc (2017).

The first survey took place on February 15, 2020 and is labelled the Red Rock Ranch line (RR). The transect line runs approximately northwest for 550 meters beginning at and moving away from the Red Rock Ranch property and following alongside Harshaw Creek. The second survey occurred on February 23, 2020 and is referred to as the Harshaw Creek line (HC). It begins to the southeast of the first line and skirts the creek heading roughly northwest for 560 meters.

Typically, DC resistivity lines are run in an array that is as straight as possible. The array that was laid out in the first weekend (RR) kept a relatively consistent bearing, until it was noted that the area of construction towards the west of the line was going to be in the way. Because of this the bearing was slightly changed so that no abrupt cornering would have to be done to get around the house in the way. Also, the manufactured flat ground would not give as reliable data providing another reason for the change in direction. The second array was found to intersect the river, and therefore the decision was made to change direction, once on the river it was realised that the river soon ran dry and to investigate the reason for this the array was chosen to follow the river's course on the bank.

4.3 Data Processing

The software used by our project partners at USGS to process these data is AGI EarthImager 2D. From the measured data, the apparent resistivities were calculated using equation (4.2) and were plotted relative to the depth of penetration from the surface to create a pseudosection that more accurately represents the measured readings (taken at 45 degrees to horizontal). The pseudosection data was then plotted against an adjustment for the ground topography to assist in the interpretation of data in relation to the field site. The measured plots, pseudosections, and topographically adjusted plots for both DC transect lines are displayed in Figures 4.3 and 4.4 below.

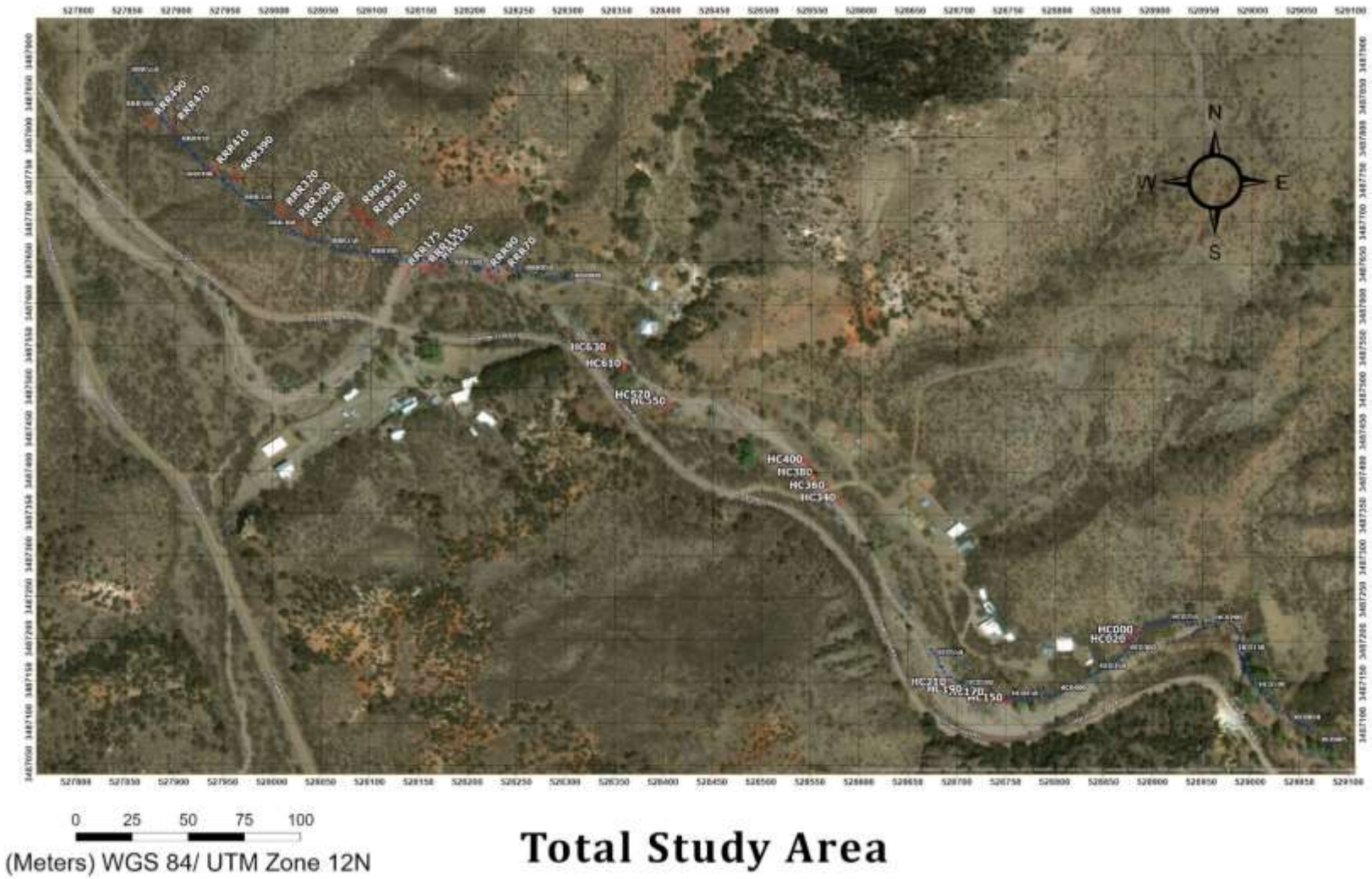

Figure 4.3. Location Map showing the position of both DC resistivity lines.

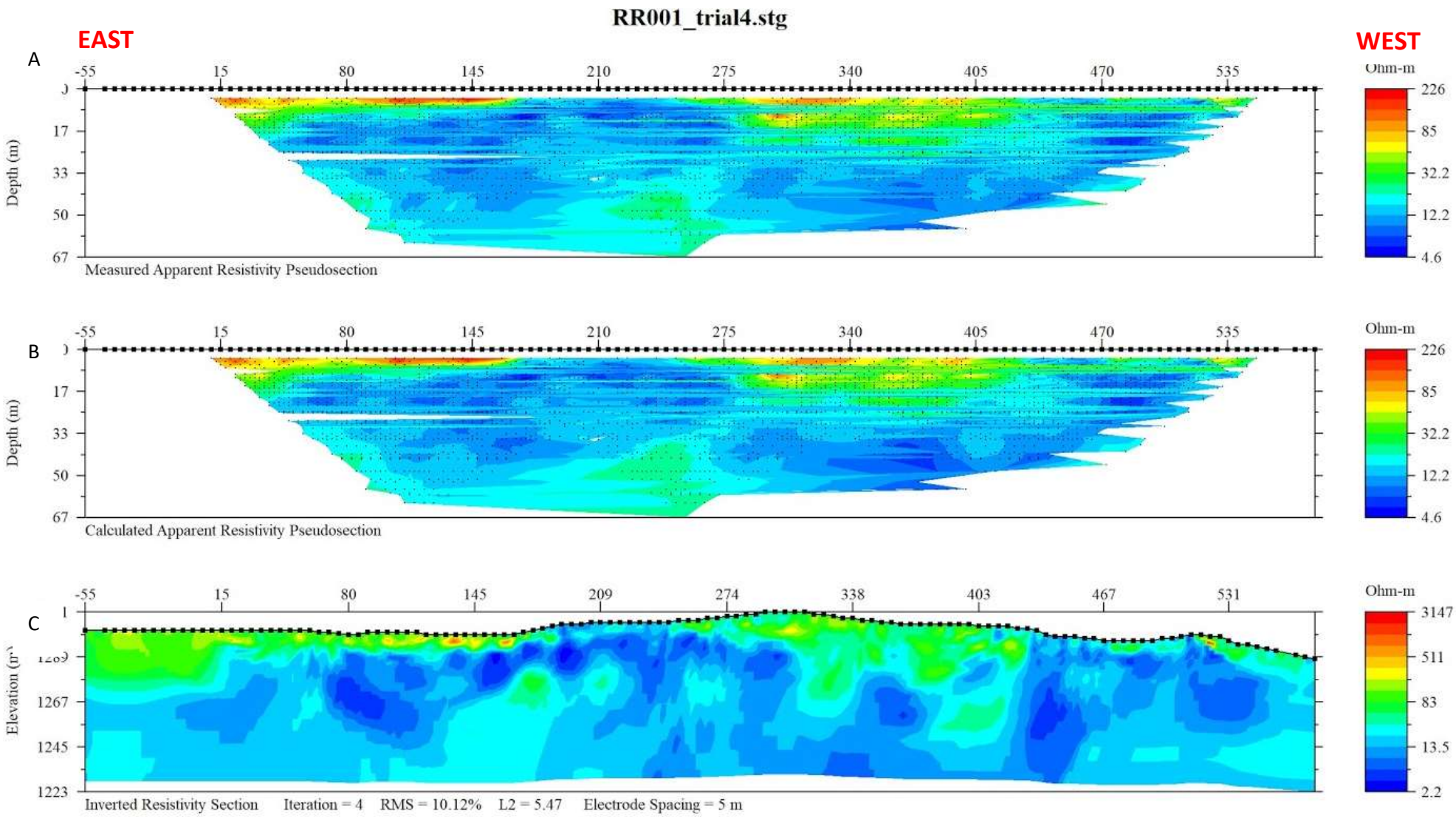

Figure 4.4. DC resistivity Data for Red Rock Ranch array.

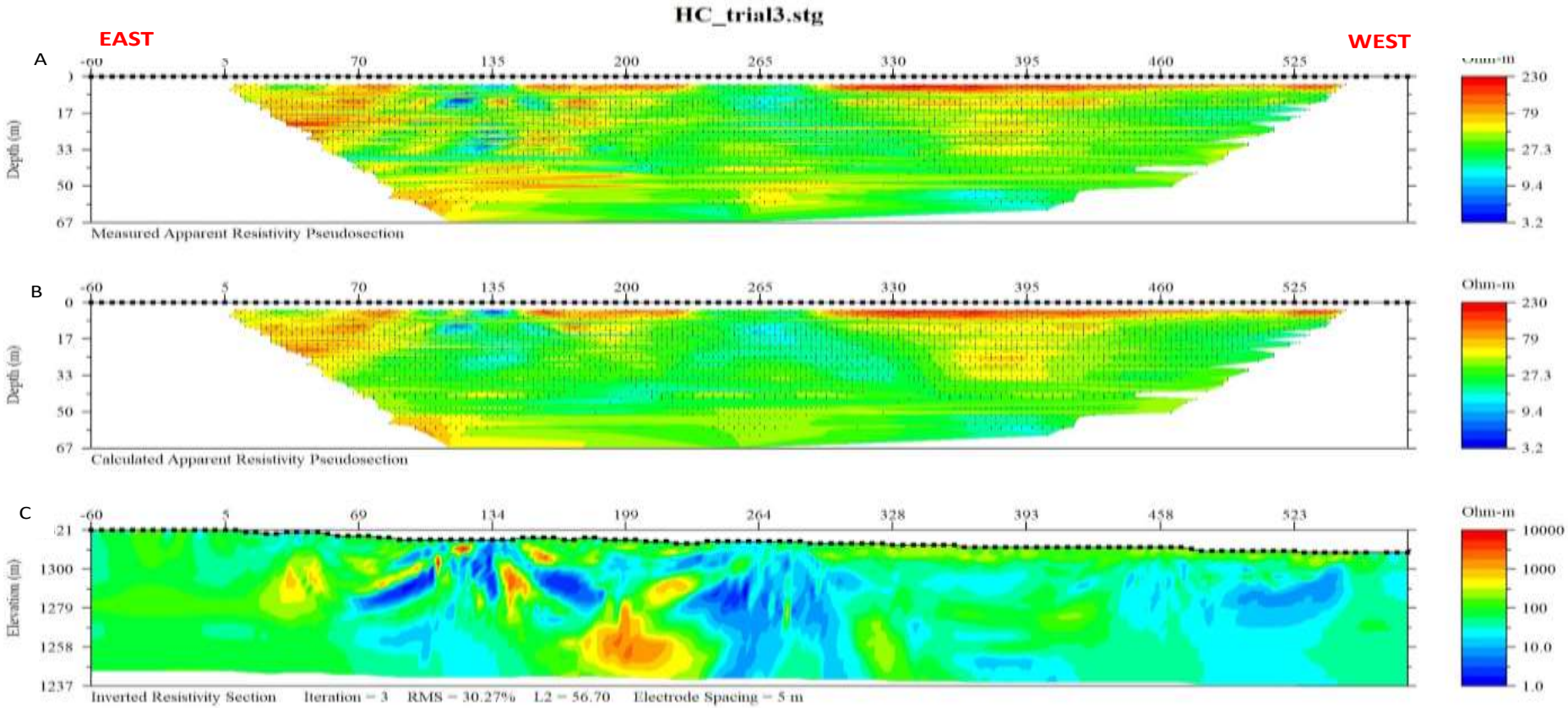

Figure 4.5. DC resistivity data for Harshaw Creek line.

4.4 Observations

The pseudosections for both surveys show some significant disagreements with the models. This is likely due to the complexity of the data collected. The measured apparent resistivity pseudosection (Figure 4.5.A) for the HC array in comparison to the model (Figure 4.5.C) shows disagreements in places. These are mostly noticed in the shallow sections, with the higher resistivity areas not being shown at the surface, and below stations 70 and 395 two patches of material in the range of 80 Ω-m stretching below the surface for about 40 m. We also see the models place two almost symmetrical structures of low resistivity below stations 134 and 264, and a point of high resistivity in the middle below station 199. None of these are apparent in the pseudosection. Points 134 and 264 were roughly near points of river crossing. The low resistivity of the water may be visible at the surface of the pseudo section. There is also a saucer shape patch of low resistivity below stations 500-550 occurring between 20 m and 40 m from the surface. This saucer is picked up on the edge of the pseudo section and then the rest inferred at the end of the survey. The RMS value for this model was at 30.27% a slightly high figure, however not too high to discount the model completely.

For the RR pseudosection and model there are less obvious disagreements between the two, the RMS value being 10.12% means a much better fit for the data here, see Figure 4.4. The main disagreement noticed here is the supressing of shallow high resistivity sections such as between stations 80–150 and 300–240 (Figure 4.4.A). The two patches of slightly elevated resistivity below stations 170 and 209 at depths of around 30 m are not seen in the pseudosections. Along the surface between stations 180 and 250 the resistivity drops to much lower values of roughly 12 Ω-m compared to the neighbouring stations recording values around 30 Ω-m. Two large patches of conductive material appear to be separated by a linear feature dipping about 45° to the east, see Figure 4.4.A.

In the HC area, the resistivity for most of the section is in the range of 30 Ω-m, whereas for the RR array they are lower, for the most part being in the range of 5-15 Ω-m.

4.5 Interpretations

The disagreements between pseudosection and the model do not appear too drastic to completely disregard the model. However, all inferences from the models without the data in the pseudosection should be backed up by other forms of data e.g. geological field observations.

4.5.1 Red Rock (RR) interpretations

Starting from the surface and working downwards, the most striking details are the patches of high resistivity, these align geographically with stations that crossed over the dry riverbed. Examples for these features are: RR80–150, HC60–95, HC150–230, HC195–550. These high resistivities can be explained with an understanding of Archie's Law (Equation 4.3). Poorly consolidated alluvium with mostly air in the pore spaces will be resistive due to the low content of water. Air being an effective insulator causes these areas to be poorly conductive, and be represented by high resistivity values that exceed 200 Ω-m. Using the pseudosections, it is estimated these layers are roughly 5 m thick for the most part.

In Figure 4.4.A it is visible that an area of lower resistivity reaches the surface. Compared to the alluvium to the east, it is noted as a conductive anomaly. This unit is inferred to be a more consolidated sedimentary rock of fluvial origin and possibly saturated with water causing the conductivity to be so elevated. For this report it will be referred to as the Red Rock Sandstone. This unit continues downwards to the east and appears to the west although separated by a linear feature of higher resistance. This unit has a thickness of roughly 40 m and is present under most of the RR pseudosection. The previously mentioned linear structure located beneath station 275 has been interpreted as a fault, due to the clear displacement of the two bodies of Red Rock Sandstone.

4.5.2 Harshaw Creek (HC) Interpretations

The HC section has a more complex structure to it, compared to the RR section, being mostly limited to a surface alluvium and the Red Rock Sandstone. The HC model has two striking conductive features beneath stations 134 and 264. They appear to share a symmetry, and due to the curved nature of the line, it is likely that this is one structure that bisects the line twice. The

trend of the feature is of a 120° bearing. Although this structure is not clearly picked up in the pseudosection, geological evidence does provide a second line of reasoning to consider this a reasonable interpretation. Continuing along strike, a continuous break-in-slope is noticed along the hills on the east side of Harshaw Creek (F. Gray 2020, personal communication, 29 March). This structure has been interpreted as a fault; a slip direction cannot be inferred from the data. However, based on the break in slope it would likely dip westwards as a normal fault. The low resistivity of the fault is likely due to increased fluid flow in this region. The brecciated nature of fault rock makes them ideal conduits for the transport of fluids. Field observations also show that the river, not too long after passing the proposed fault, runs dry. This may be due to the increased permeability in the subsurface providing a preferred route for the water to flow.

The point of high resistivity below station 199 (Figure 4.5.c), which is not seen in the pseudosection has questionable validity. The absence of this feature in the pseudosection does raise concern, although it is located perpendicular to a hill of basalt (Figure 4.4). This basalt would possess a high resistivity and likely continues below the section.

The final two areas of interest are the point of high resistivity below station 395 and the saucer shaped feature beneath stations 500-550 occurring between 20 m and 40 m from the surface. These two will be discussed further in the conclusions section.

4.5.3 Local Area

As mentioned in the observation section, the HC data have a higher relative resistivity when compared to the RR data. This could be pinned down to one of two reasons, both using Archie's law (Equation 4.3) Firstly, the saturation of the subsurface may be causing this discrepancy. Faulting in the area, with anomalously low resistance, may represent a preferred route for groundwater migration. This would lead to less saturated geology, which would increase the resistivity of the surrounding geology. Alternatively, the difference could be the result of a change in resistivity of the water that is percolating through the subsurface. A fluid that has assimilated more metals and ions will be more conductive and therefore create a lower resistivity signature in the data. In this case, between the HC and the RR areas, ground water has come into contact with a contaminating body. This second rationale is complemented by the slight gradient

in resistivity that increases in both models towards the west, although option 1 is still possible. In reality it is likely to be a mixture of the two theories contributing to this detail.

4.6 Possible Future Work

Figure 4.6 summarizes the location of existing data. The green lines represent proposed future TEM and DC resistivity lines. These lines could provide more resolution of the geologic anomalies discussed in this report.

Figure 4.6. Positions of the Red Rock (red) data and the Harshaw Creek (blue) data represents the location of existing data. Green lines represent recommended future resistivity lines.

4.7 References

Advanced Geosciences Inc., 2017, Dipole-Dipole Array: Electrical Resistivity Methods, Part 3. (2019, May 31). Retrieved April 10, 2020, from https://www.agiusa.com/dipole-dipole - array

Wightman, W. E., Jalinoos, F., Sirles, P., & Hanna, K. (2016, May 18). Resistivity Methods. Retrieved April 10, 2020, from https://archive.epa.gov/esd/archive-geophysics/web/html/resistivity_methods.html

5. GEM-2 Frequency Domain Electromagnetic (FDEM) Surveys

5.1 Introduction

The GEM-2 is a geophysical electromagnetic survey device created by the company Geophex. Unlike the TEM geophysical survey, the GEM-2 system operates via Frequency Domain Electromagnetics (FDEM). A sinusoidal wave is created by a transmitter at the back end of the device, which is then buffered by a bucking coil in the middle of the device to prevent the device from receiving its own transmitted frequency. The receiver coil at the front of the GEM-2 system then picks up induced signals in the earth for the specific frequency. The data are presented as in-phase ppm and quadrature ppm values. These in-phase and quadrature ppm values then allow for interpretation of the conductivity of near-surface anomalies.

The overall device is approximately 1.8 meters long and suspended horizontally above the survey area by a shoulder strap attached to the operator. Due to its length, the GEM-2 device is often referred to as “the ski” by field personnel. The on-board computer is attached to a portable GPS unit, which allows the GEM-2 to record position values while the survey is underway. Although the unit has an on-board computer, there is no user interface on the GEM-2, requiring the device to be paired via Bluetooth to a control system, most often a hand-held computer, where data logging can be controlled and read immediately by the operator.

The GEM-2 can be used to record many different frequency data on one collection run as well as many cycles of data, allowing for the stacking of data. The lower frequency values (often under 4000 Hz) are susceptible to large amounts of noise, with higher definition in the upper ranges, usually above 6000 Hz. After data collection, the data are available via CSV files, which contain the GPS data as well as the FDEM results in parts per million of in-phase and quadrature. These data can then be manipulated in data-processing software, such as Excel, MATLAB or R.

5.2 Field Procedures and Instrumentation

Data were collected with the GEM-2 system on February 15th and 16th, 2020, with most of the data processing occurring on site or en route to the survey location on February 22nd and 23rd, 2020. While the GEM-2 from Geophex can be used in either a "horizontal" or "vertical" sense for ease of use by the operator, the survey was conducted using the "horizontal" orientation as a means of ensuring that the device was held completely parallel to the surface of the Earth. With the help of a spotter (D. Xavier), the operator (K. W. Brown) was able to ensure proper orientation of the ski for the duration of both runs. For this survey, two runs were completed along the Red Rock Ranch line, between meter markers 0 and 260 parallel to the DC resistivity survey line. The GEM-2 was kept at waist level by the shoulder strap on the ski, and the operator moved along the line following the DC resistivity survey conducted in the area with the guidance of her spotter. The terrain was quite uneven, with the survey line dropping one meter into a wash and climbing about 2 meters vertically out of it.

The GEM-2 collected FDEM data on five different frequencies (450, 1530, 5310, 18330 and 63030 Hz) for this survey and operated on a limited range of 260 meters to ensure adequate battery charge for the on-board computer within the ski. A Garmin GPS receiver was attached to a wide brimmed hat and worn by the operator, and a hand-held computer was used by the spotter to assure correct data collection during the survey. To start each line, specific "codes" were agreed upon by the survey team so that the data could be recognized on the hand-held computer and prepared for export. These codes were generated by moving a shovel under the receiver of the ski several times to mark the start of true data collection, and a section of wire fence was used in a similar manner to mark the end of true data collection.

Figure 5.1: Geophex GEM-2 Ski Demonstration, Courtesy of Geophex Ltd.

5.3 Data Processing

The data collected on both runs with the GEM-2 system were processed and analyzed predominantly while in-field on the weekend of February 22nd and 23rd, 2020. The data were originally compiled by the GEM-2 on-board computer in UTM coordinates with no information available for distance. This required a small calculation to generate the distance between the start of the line and the current point. This function is the general distance function, as UTM coordinates are presented in meters Easting and Northing. The distance values proved vital to later interpretation, as the DC resistivity and TEM surveys in the area had data available in distance from the start of the line rather than pure UTM coordinates.

Once distance values were calculated for both runs in Excel, the in-phase and quadrature ppm values were plotted with respect to the distance from the start of the line. This allowed for two series of graphs for interpretation: the first showing changes of in-phase ppm over distance, and the second showing changes of quadrature ppm over distance. The line in question runs closely parallel to the DC resistivity line for the Red Rock Ranch survey, with a horizontal deviation between 3 and 5 meters from the DC line.

5.4 Interpretation

Upon processing, the data showed two anomalies: a small anomaly around the 40 meter mark (visible in the quadrature ppm graphs), and a larger anomaly around the 180 meter mark (visible in both the in-phase and quadrature ppm graphs). This prompted in-field investigation to remove the posibility of a false positive. This was done by inspecting a 10 meter radius circle around each anomalous area for the presence of any metal fragments that could potentially cause an anomaly. After confirming that there was no metal present at either location, it serves to reason that the areas in question have a relatively high conductivity (a low resistivity) in the near subsurface. Based on the size of disturbance between the two anomalies, the 40 meter mark location has a lower conductivity than the 180 meter mark location, but both regions were more conductive than the rest of the survey areas.

The anomaly at the 180 meter mark served as basis to add a TEM loop at the 175 meter mark to increase definition in the TEM pseudosection for the Red Rock Ranch survey area. Based on the TEM and DC resistivity survey information for the 180 meter mark, it is visible that there is a region of measured lower resistivity in the near subsurface (i.e. 5-20 m depth). This also corresponds with a smaller region of lower resistivity at the 40 meter mark in the DC resisitivity survey at a slightly larger depth (approximately 20-25 meters). Based on these data, it can be interpreted that the two zones most likely contain more hydrated clays than the surrounding regions, and therefore have a lower resistivity than the rest of the survey area. Due to metal content in the water near Harshaw Creek, the water itself is somewhat conductive. When this water is bound in sediment layers, such as clays, the conductivity increases, causing a local anomaly in the GEM-2 data.

Although there is a concentrated anomaly at the 180 meter mark, the in-phase and quadrature ppm values remained higher than the rest of the survey area beyond the 180 meter mark. This corresponded to an increase in elevation of about two meters on the other side of a wash, as well as a consistent zone of lower resistivity on the DC resistivity survey for the area. Based on these combined data, the presumptive clay zone along the 180 meter mark runs at least 30-40 meters past the initial large anomaly, at a depth between 5-20 meters. It is unlikely that the water table is at this level, as local well data shows an average well depth of approximately 30-35 meters

(USGS, 2020). There is a small chance that there may be a perched aquifer in the near subsurface, but due to surrounding geology, it is more likely that the area of low resistivity around the 180 meter mark (as well as the 40 meter mark) is caused by water flow through rocks above the clay layer.

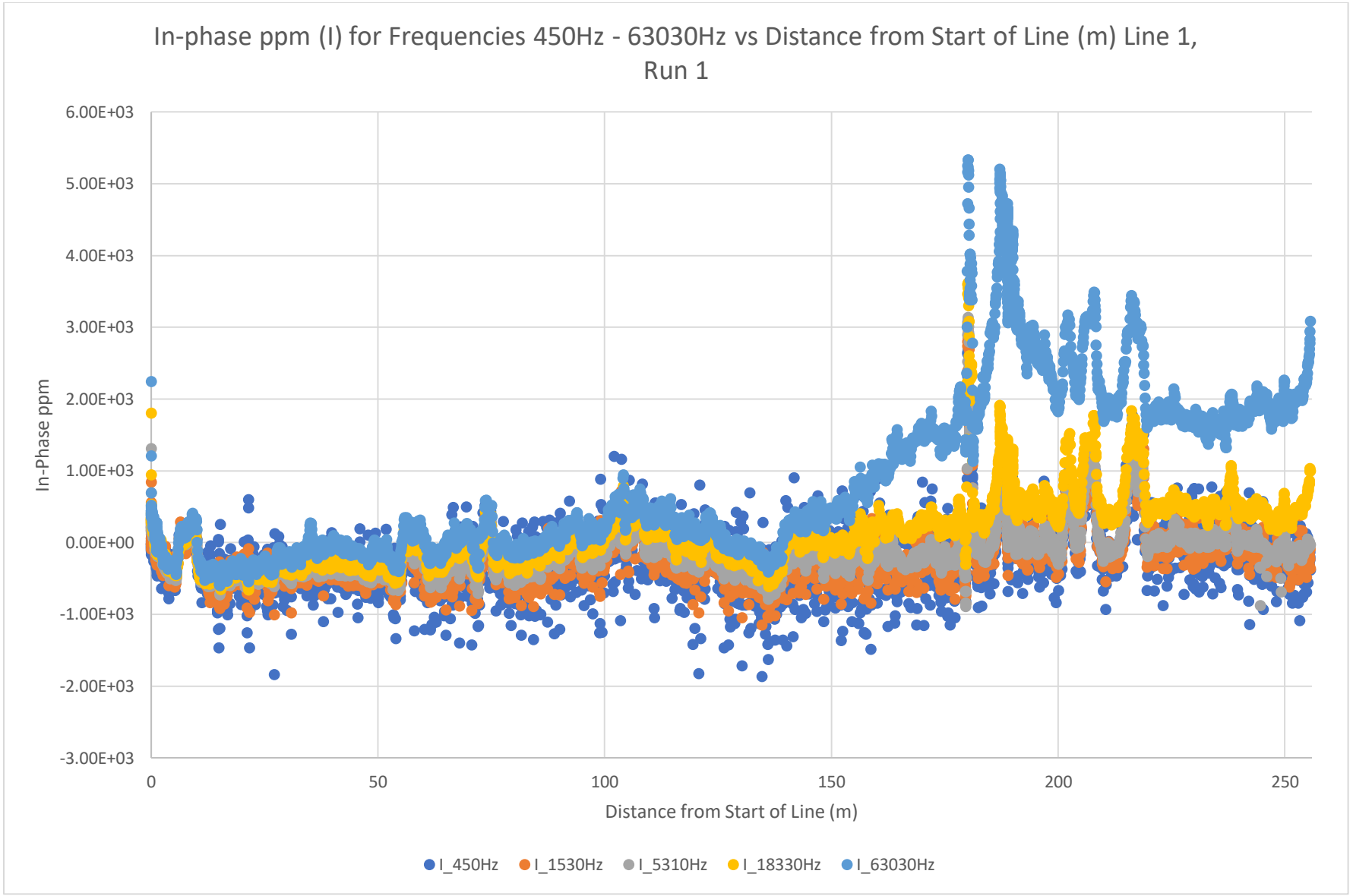

Figure 5.2: In-phase ppm Data for the first run.

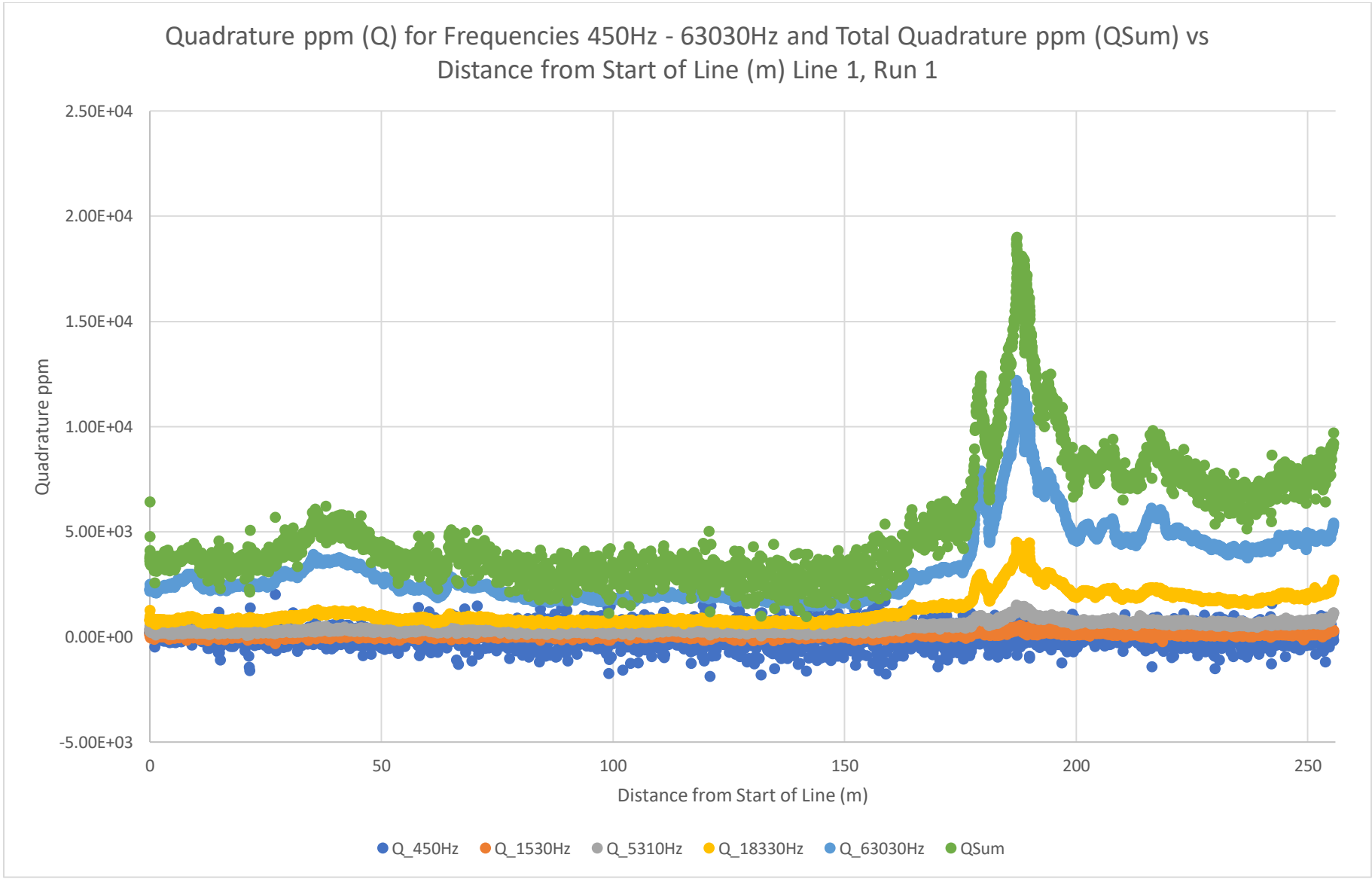

Figure 5.3: Quadrature ppm data for the first run.

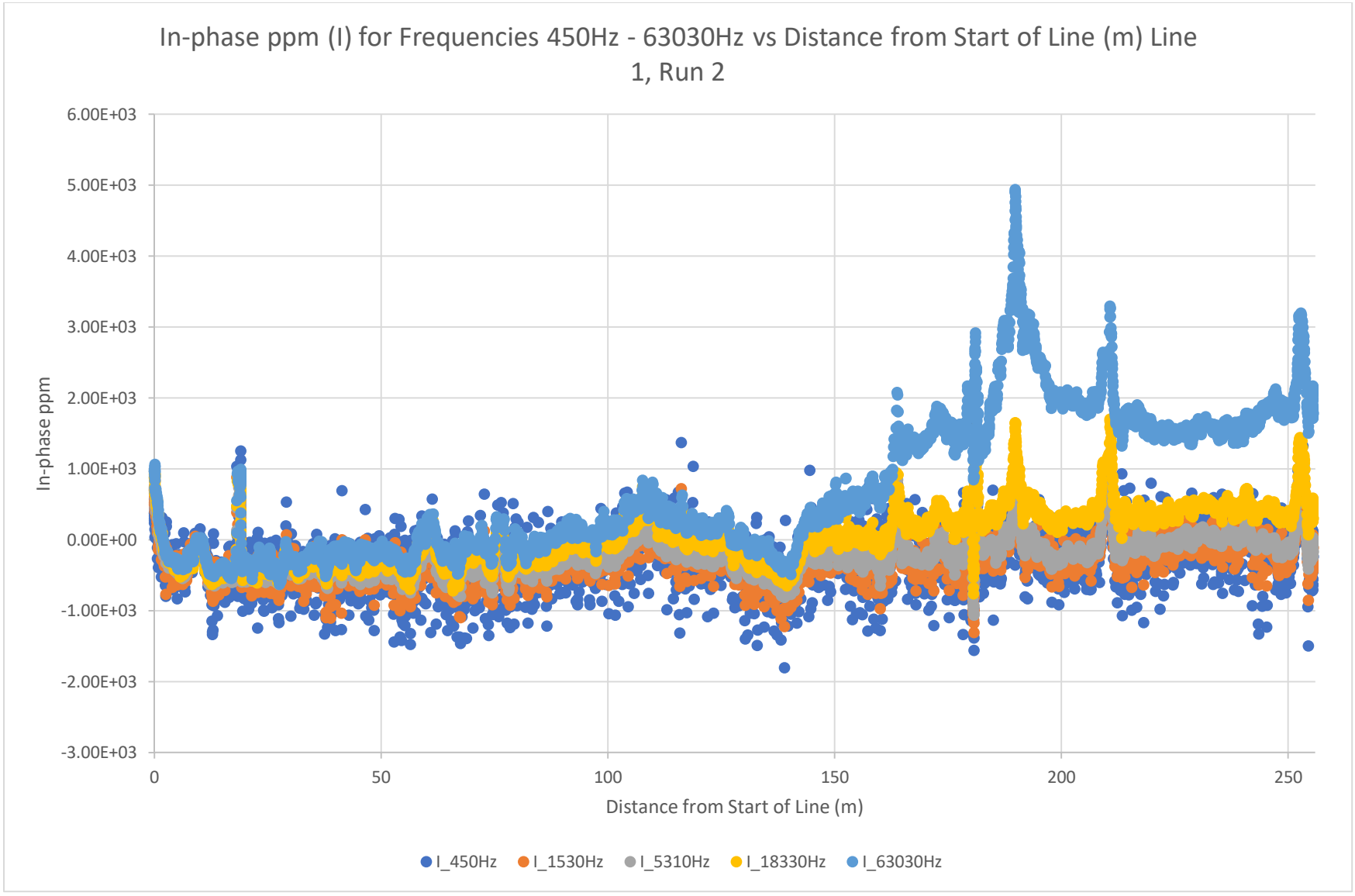

Figure 5.4: In-phase ppm data for the second run.

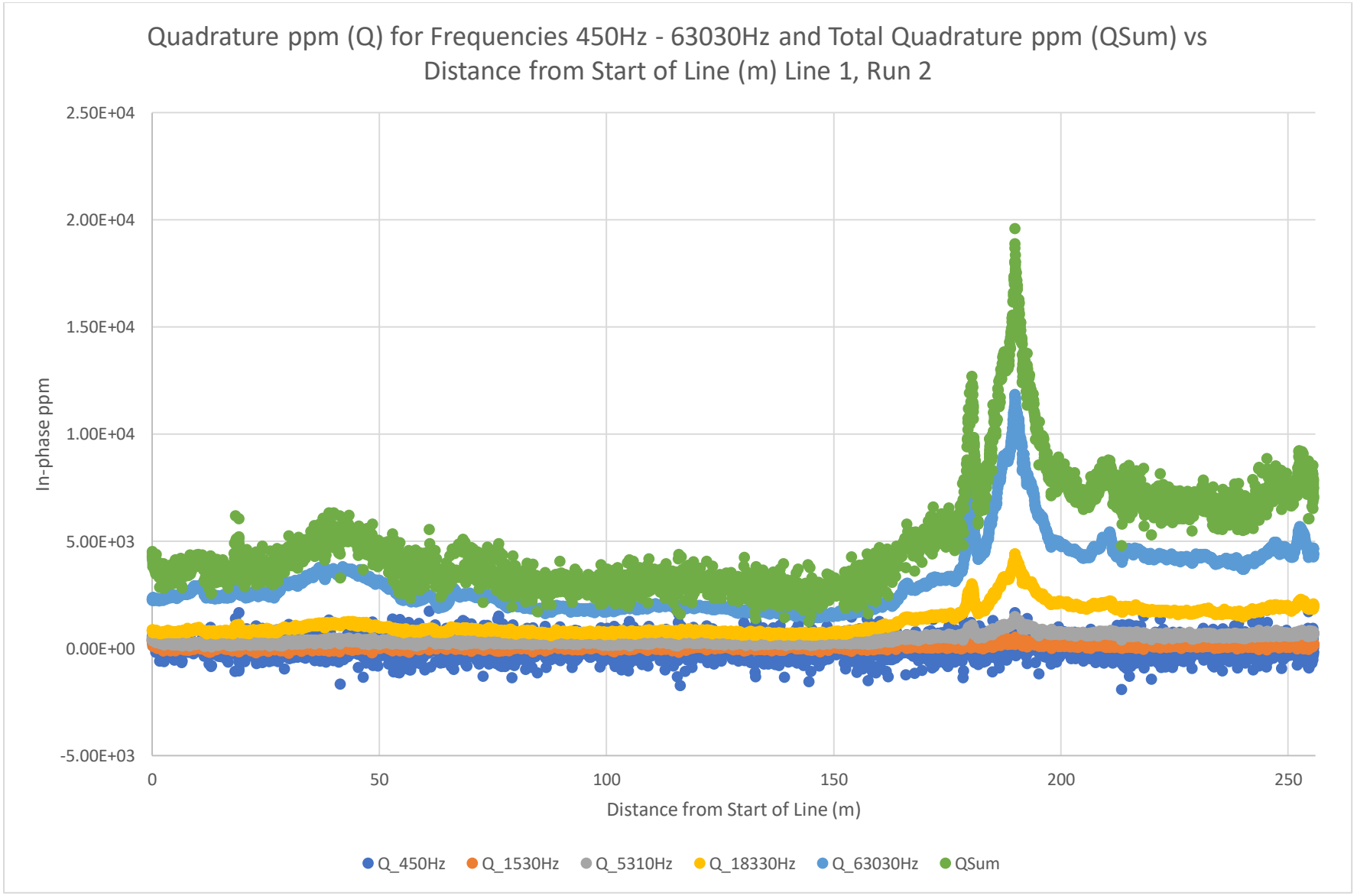

Figure 5.5: Quadrature ppm data for the second run.

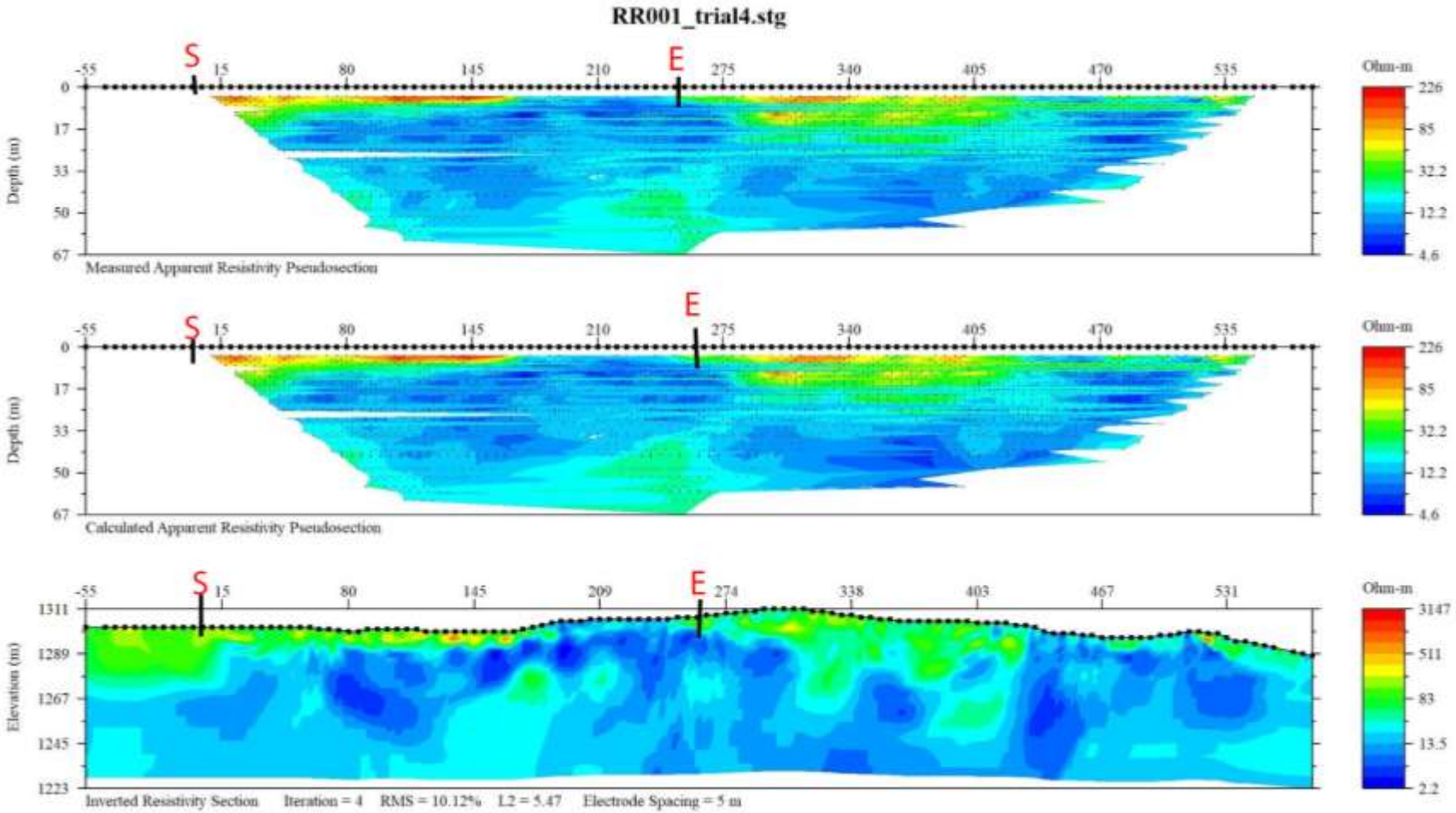

Figure 5.6: The DC resistivity pseudosections and model used for comparative analysis. The start (S) and end (E) of the GEM-2 line is marked in red above.

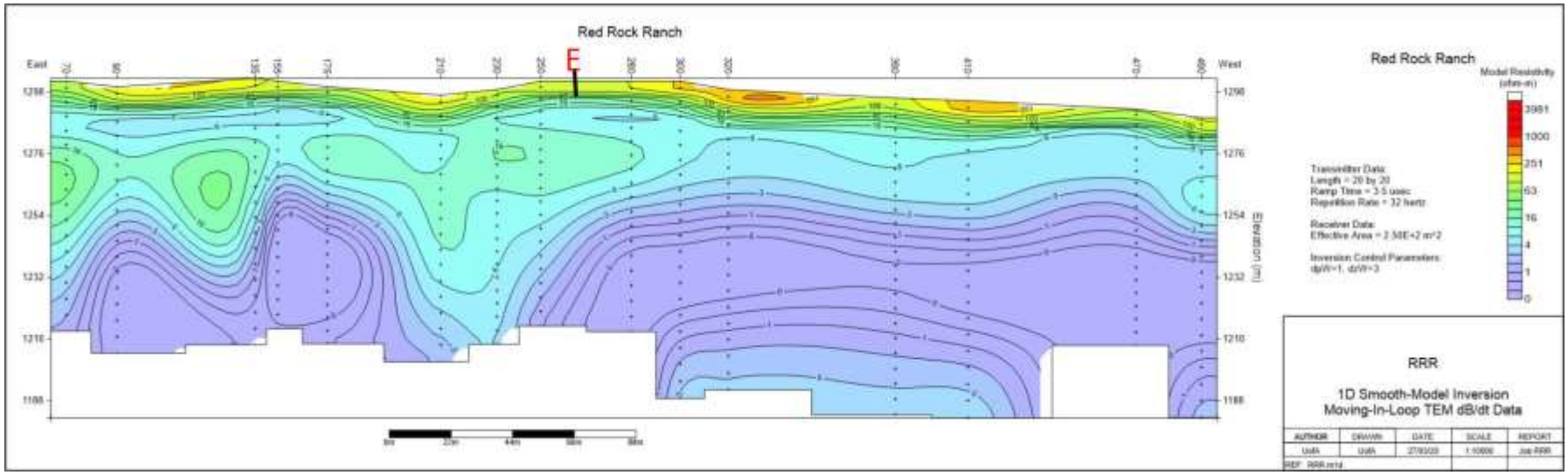

Figure 5.7: The TEM pseudosection used for comparative analysis. The end of the line (E) is marked in red above.

5.5 References

Geophex Ltd., Hand-held Gem-2 Ski, http://www.geophex.com/Product_GEM2_handheld.htm, accessed March 31, 2020.

Gray, Floyd, 2020, Lower Harshaw Creek: Red Rock Ranch – Peterson Homestead: Presented to GEN/GEOS 416/516 Class, Spring 2020.

6. Combined Analysis

6.1 Methods

To adequately interpret the cross sections produced from both the TEM and DC Resistivity sections it was important to first allign them. Due to a lack of field time there is only a small overlap in the data for the HC area, however it has been enough to substantiate our results. Using Figure 6.1 we aligned the cross sections to the best of our abilities, as the lines are not perfectly straight and they deviate from each other in several places, the numbers will not match up perfectly e.g. TEM 210, 230 and 250. Due to the terrain, it was not possible to place the TEM squares loops along the already completed resistivity line, and therefore a decision was made to move it as close to the array as possible. Figures 6.2 and 6.3 are the aligned cross sections. They both use the same key that is shown on Figure 6.3.

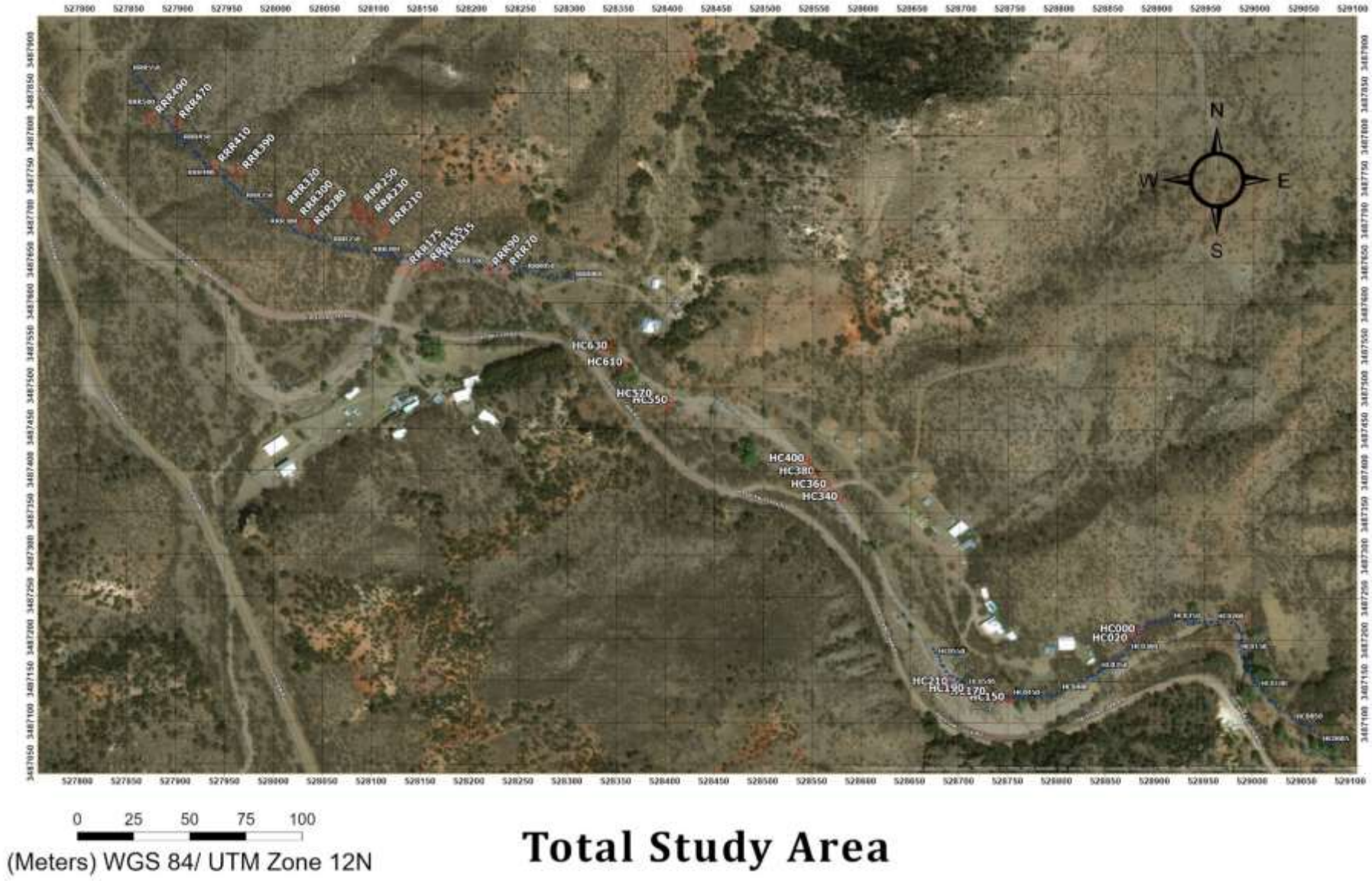

Figure 6.1 Location map used to align the cross sections from the two different types of data. These is a clear offset in the TEM and Resistivity cross sections in the HC area.

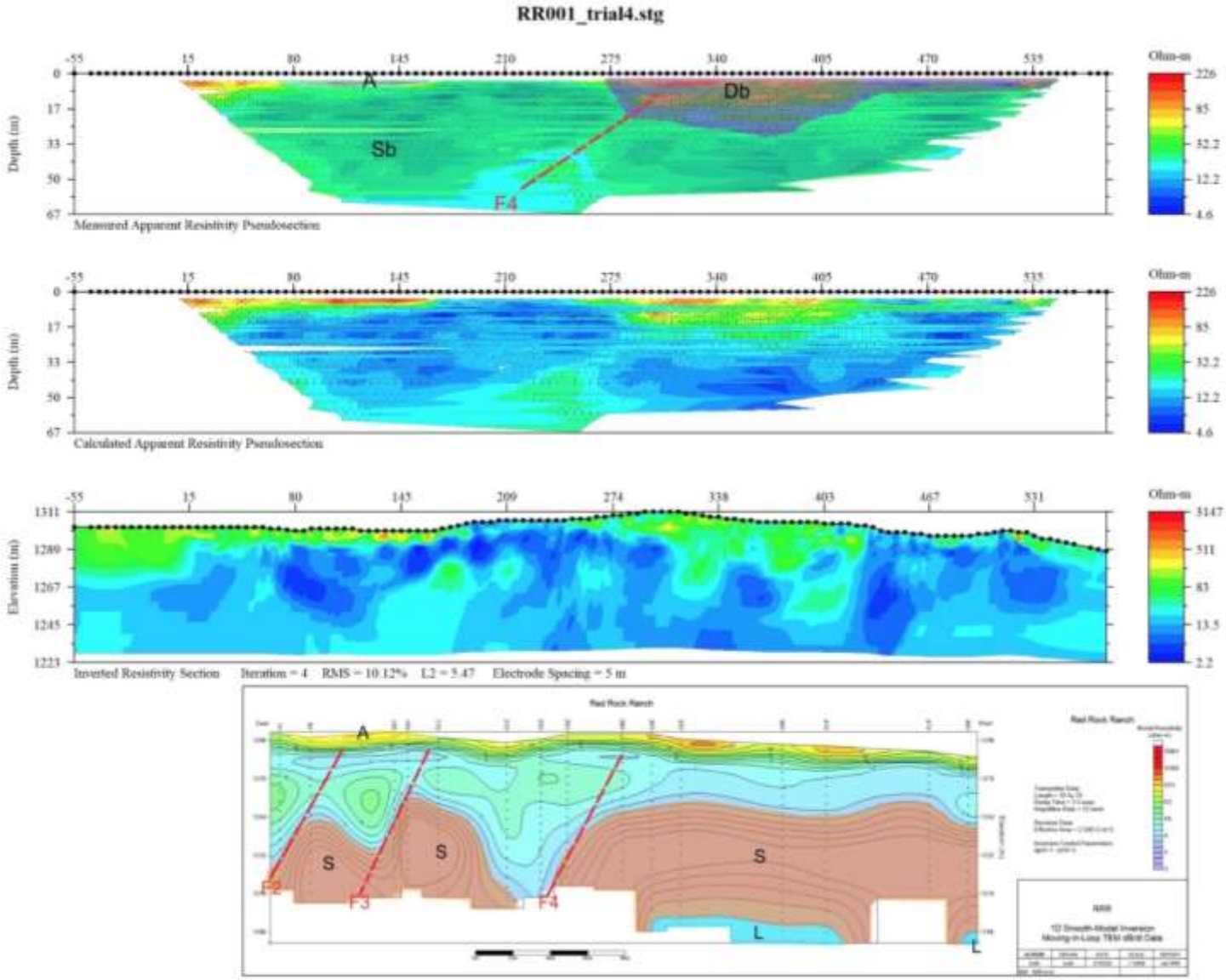

Figure 6.2 The Aligned cross section for the Red Rock Ranch profiles of data.

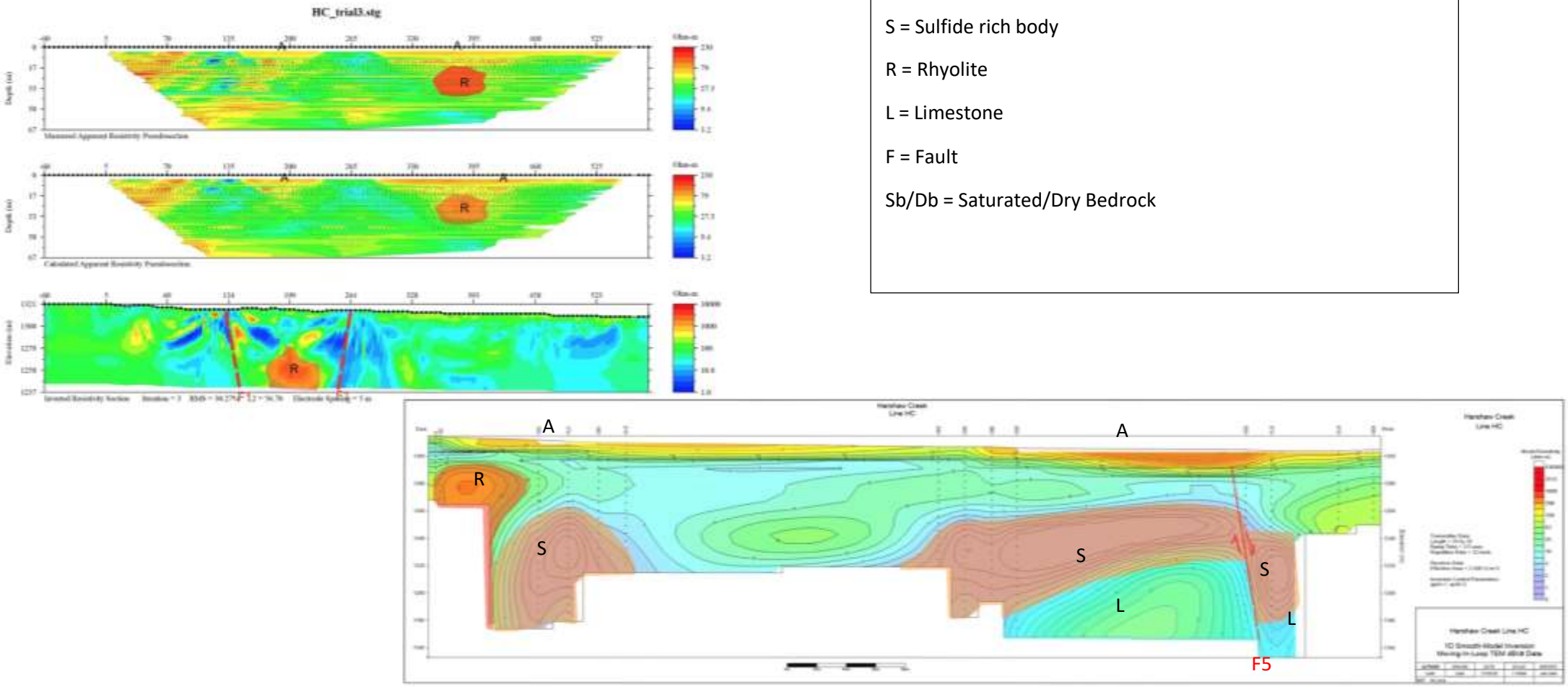

Key

A = Alluvium

S = Sulfide rich body

R = Rhyolite

L = Limestone

F = Fault

Sb/Db = Saturated/Dry Bedrock

Figure 6.3 The aligned cross sections for the Harshaw Creek profiles of data.

6.2 Interpretation

Since the GEM-2 method has a limited depth of investigation, in comparison with the TEM and DC Resistivity methods used here, and since the GEM-2 interpretation has already been discussed in the previous chapter, we will not be discussing these data extensively here. At the 180 mark along the GEM 2 data, an area of low resistivity is seen that correlates very well with the resistivity data, this feature likely represents the change from alluvium to a more conductive geological unit, that may have been more hydrated.

By comparing the DC resistivity and the TEM data, some important correlations can be made. Although the data from the two methods disagree in places, the data sets are deemed complimentary, with TEM providing deeper investigation (up to 120 m) and DC resistivity shallower (up to 50 m).

The models and pseudosections from the resistivity data do not align perfectly, they both provide good data that has been interpreted to form different parts of the overall understanding for the subsurface geology. The highly resistive features at the surface were picked up best on the measured pseudosections (Figure 6.2 and 6.3) but did not appear in the model to the extent they ought to have been. These features for the most part were geographically associated with the areas of dry alluvium. These points typically had resistivities above 200 Ω- m.

The task to find the cause of the non-potable water below the Red Rock Ranch, has been met. This study finds that sulfide rich bodies, characterised by anomalously low resistivity, is the likely cause. Upstream along Harshaw Creek, the Rocking Chair Ranch has potable well water, however 500 m away, it is acidic and contains elevated concentrations of dissolved metals. The TEM methods picked up the low resistivity bodies at depths of roughly 30–40 m. The bodies had an average thickness of 40 m. Extensional normal faulting has caused certain parts of the sulfide rich body to subside and it is now found at deeper depths. Below the Red Rock Ranch, the depth of the body is at its most shallow, being less than 30 m from the surface (Figure 6.2). The resistivity data adds a second line of evidence with the slight increasing gradient in average conductivity of the subsurface from west to east (Figures 6.2 and 6.3). This is caused by the

number of dissolved ions increasing to the west as more groundwater has interacted with the sulfide minerals.

The interpretation of limestone units beneath the sulfide rich body comes from the hypothesis that the deposits located in the research area are skarn type deposits. This inference has been made by seeing similar findings in the South 32 minerals declaration report (South32, Ltd., 2020).

A second alternate theory for this gradient, although less favored, is that this gradient is produced by a differential in saturation of the bedrock. Both theories use an understanding of Archie's Law, however, focus on separate aspects. The faulting in Figure 6.3 is so conductive that it is possible the flow of water in the subsurface has been concentrated into Fault 1. This leads to a lower saturation in the surrounding geology, whereas in the Red Rock Ranch area the water has dispersed into the rock more, raising the saturation and with it the conductivity.

From the TEM and DC Resistivity data, we have identified five faults along the section of study, labelled F1 through F5, all of which were normal faults. These extensional faults likely formed during the extension of the Cordilleran Orogeny during the Cenozoic. Fault 4 shown in the resistivity data in Figure 6.2 looks like a reverse fault, however the units separated are not geological units, instead they are just saturated versus dry bedrock and likely have no connection to a lithological change.

6.3 Reference.

South32, Ltd., 2020, HERMOSA PROJECT - MINERAL RESOURCE DECLARATION: https://www.south32.net/docs/default-source/exchange-releases/hermosa-project---mineral-resource-declaration.pdf?sfvrsn=9a2536d6_2, accessed 4/30/2020.